AD NUMBER
AD355503
CLASSIFICATION CHANGES
TO: unclassified
FROM: confidential
LIMITATION CHANGES
TO: Approved for public release, distribution unlimited
FROM: Distribution authorized to U.S. Gov't. agencies and their contractors; Administrative/Operational Use; NOV 1964. Other requests shall be referred to Air Force Aero Propulsion Lab., Wright-Patterson AFB, OH 45433.
AUTHORITY
AFWAL ltr, 22 Dec 1983; AFWAL ltr, 22 Dec 1983

AD 355503

ADVANCED AIR BREATHING ENGINE STUDY

Technical Documentary Report No. APL TDR 64-112

November 1964

AIR FORCE AERO PROPULSION LABORATORY
RESEARCH AND TECHNOLOGY DIVISION
AIR FORCE SYSTEMS COMMAND
WRIGHT PATTERSON AIR FORCE BASE, OHIO

Project 3012 Task 301201

Prepared under contract No. AF33(657)-10794

by

National Engineering Science Company
711 S. Fair Oaks Avenue
Pasadena, California

Authors: R. Kushida, Ph.D., F. Falconer and D. Seiveno

NOTICES

When Government drawings, specifications, or other data are used for any purpose other than in connection with a definitely related Government procurement operation, the United States Government thereby incurs no responsibility nor any obligation whatsoever; and the fact that the Government may have formulated, furnished, or in any way supplied the said drawings, specifications, or other data, is not to be regarded by implication or otherwise as in any manner licensing the holder or any other person or corporation, or conveying any rights or permission to manufacture, use, or sell any patented invention that may in any way be related thereto.

This document contains information affecting the National defense of the United States within the meaning of the Espionage Laws, Title 18, U. S. C., Sections 793 and 794. Its transmission or the revelation of its contents in any manner to an unauthorized person is prohibited by law.

Qualified requesters may obtain copies of this report from the Defense Documentation Center (DDC), (formerly ASTIA), Cameron Station, Bldg. 5, 5010 Duke Street, Alexandria, Virginia, 22314.

Copies of this report should not be returned to the Research and Technology Division, Wright-Patterson Air Force Base, Ohio, unless return is required by security considerations, contractual obligations, or notice on a specific document.

FOREWORD

This report was prepared by the National Engineering Science Company, (NESCO), Pasadena, California, on Air Force Contract No. AF 33(657)-10794, "Advanced Air-Breathing Engine Study." The work was administered under the direction of the Research and Technology Division, Wright-Patterson Air Force Base, Ohio. Mr. Ruben Canny was Project Engineer for the Research and Technology Division.

The studies on the present program were initiated on 6 March 1963 and are continuations of analytical investigations done at NESCO under Air Force Contract No. AF 33(616)-8506 and AF 33(657)-9244. Dr. Raymond Kushida was the program manager for NESCO.

The advice and technical direction of Dr. Ernest Mayer, Associate Director, Science Division and Dr. G. V. R. Rao, Assistant to the President, Propulsive Systems (NESCO), are gratefully acknowledged.

This report is the Final Report on Contract AF 33(657)-10794. The contractor's report number is SN/129.

This report is classified "Confidential" because it contains data on cycle description, engine and component performance, and engine and component operating conditions pertaining to advanced air-breathing engines.

ABSTRACT

This report summarizes analytical studies on supersonic combustion ramjet engines. The performance capabilities of components, such as inlet, combustor, and exit nozzle, are studied from theoretical considerations and their influence on the engine performance is examined. Turbulent mixing in combustor, nozzle flows with nonuniform entrance, incomplete recombination within the nozzle, and the influence of nozzle contour are included.

This abstract is unclassified.

This Technical Document has been reviewed and approved

TABLE OF CONTENTS

TABLE OF CONTENTS (continued)

ILLUSTRATIONS

ILLUSTRATIONS (continued)

ILLUSTRATIONS (continued)'

TABLES

1.0 INTRODUCTION

The purpose of the Advanced Air-Breathing Engine Study is to conduct analytical investigations of means to optimize the propulsive potential of the hydrogen fueled supersonic combustion ramjet engine. This is the Final Report on this study.

This report has been organized so that each section is essentially complete within itself. References and figures pertaining to a particular section will be found at the end of each section.

Manuscript released by the author 4 August 1964 for publication as an RTD Technical Documentary Report.

2.0 SUMMARY

The study of component performance and their effect on the over-all thrust performance of the supersonic combustion ramjet engine is clarified by explicit use of the "impulse function" as a variable rather than pressure velocity, enthalpy, or temperature. Consequently, the nonuniformity at the combustor entrance due to realistic inlet configurations is shown to be of secondary importance as far as its effect on the over-all performance is concerned. It is believed that the use of the impulse functions will lead to significant simplification in the application of theoretical computations and interpretation of experimental data to the design and performance evaluation of engines.

The experimental data on penetration of fuel injection into a supersonic stream could not be correlated with theory based on subsonic experience. Supersonic theories which do correlate the experimental data call for much smaller penetrations.

The integral equations of motion for turbulent compressible mixing with equilibrium reaction were used for the study of Scramjet combustion. Mixing in variable area ducts is studied. Release of heat due to combustion shortened the flame length. Constant area ducts required a shorter distance for the same amount of mixing compared to divergent ducts. Simulated shock losses on the air side of the mixing region caused the turbulent shear to decrease, leading to a longer combustor.

The thrust delivered by the divergent portion of the exit nozzle is studied with variation of nozzle configuration parameters. For a

nozzle of given exit area the influence of wall friction leads to an optimum length beyond which the performance is reduced. The influence of nonuniform flow conditions at the nozzle entrance and incomplete recombination within the nozzle are examined for a specific configuration. It is shown that these losses, even though dependent upon the flow field obtained in the nozzle, can be estimated from a quasi one-dimensional analysis.

3.0 ON SCRAMJET CYCLE ANALYSIS

3.1 INTRODUCTION

Parametric analysis of the performance potential of supersonic combustion ramjets (Scramjets) by several groups (Refs. 1, 2, & 3)* demonstrate the sensitivity of the net thrust on component efficiencies. The strong interdependence of the component efficiencies and the over-all thrust prevents a ready untangling of the relative importance of the various physical loss phenomena. In the present analysis, the engine cycle is analyzed using the impulse function. Concise and fundamental insight into the loss processes in the Scramjet is thereby obtained.

3.2 LIST OF SYMBOLS

		Units
A	Area	ft^2
C_D	Diffuser Internal Drag Coefficient	--
C_{Ej}	Impulse function Efficiency	--
C_V	Velocity Coefficient	--
D	Drag	lb_f.
D	Hydraulic Diameter	ft.
F	Force, Thrust	lb_f.
f	Fuel-to-Air (Mass) Ratio	--
f'	Chemical Heat Release Fuel-Air Ratio (For $f \leq f_{stoich}$, $f' = f$; for $f \geq f_{stoich}$, $f' = f_{stoich}$)	--

* Subject references appear in Section 3.11, page 37.

LIST OF SYMBOLS (continued)		Units
f_c	Combustor Friction Factor	--
h	Enthalpy	Btu/lb
I_{sf}	Fuel Specific Impulse	lb_f-sec/lb_m
j	Specific Impulse Function	ft/sec or lb_f- sec/lb_m
K	Kinetic Energy Conversion Efficiency	--
L	Length	ft
M	Mach Number	--
$\dot{m}$	Mass Flow	lb_m/sec
P	Pressure	lb_f /ft^2
q	Dynamic Pressure	lb_f /ft^2
s	Entropy	Btu/lb-^oR
S	Surface Area	ft^2
V	Velocity	ft/sec
α	Direction Cosine Angle	rad
γ	Ratio of Specific Heats	--
η_C	Combustion Efficiency	--
η_{KE}	Kinetic Energy Efficiency	--
η_P	Static Pressure Recovery Efficiency	--
λ^o_f	Fuel Lower Heating Value	Btu/lb_m

Subscripts

C	Combustor
D	Diffuser
f	Fuel

Subscripts (continued)

i	Ideal, Isentropic
int	Internal
N	Exhaust Nozzle
t	Total, Stagnation
0	Free Stream, Ambient
2	Diffuser Exit (Combustor Entrance)
3	Fuel Injection Station
5	Combustor Exit (Exhaust Nozzle Entrance)
6	Exhaust Nozzle Exit

3.3 GENERAL DISCUSSION

One of the primary factors which distinguish Scramjet cycle analyses from the conventional subsonic combustion ramjet cycle analyses is the use of a momentum balance around the combustor in order to obtain the combustor exit velocity and pressure. In conventional ramjets the combustor exit velocity is determined by the exhaust nozzle sonic throat condition, hence is primarily a matter of energy balance. The pressure at the sonic throat on the other hand is determined by the inlet pressure ratio. The coupling between pressure ratio and throat velocity is relatively weak, so that for a given combustor, the thrust can be directly related to the inlet performance alone. In a Scramjet however, the combustor exit velocity and pressure are strongly dependent on each other and the role of inlet performance is not clear-cut. Another way to look upon the

inlet is primarily as a means of modifying the stream thrust rather than as a thermodynamic process. The use of internal drag coefficients rather than entropy rise as a measure of losses suggests itself. Evaluation of gas properties can then be avoided in approximate analyses at least to the nozzle expansion process, since the drag coefficients already reflect real gas effects.

The use of various measures of entropy rise due to irreversible losses in the Scramjet diffuser has lead to a number of highly arbitrary modifications of conventional efficiency parameters. For the sake of convenience in computation, the kinetic energy conversion efficiency, K_D, and the pressure recovery efficiency η_P have been used in place of the more conventional kinetic energy efficiency η_{KE} and total pressure ratio. Since the entropy rise must be interpreted in terms of thermodynamic state variables such as temperature, pressure, enthalpy, and density, various definitions of the "correct average state properties" have been advanced for situations where the flow is highly nonuniform. Entropy changes occur due to both viscous dissipation (in boundary layers and in shock waves) and heat losses, while stream thrust changes occur only due to forces acting on the control surface (body forces such as bouyancy are negligible). Arbitrary definitions of efficiency parameters are introduced to insure, in an approximate manner, that the parameter applies to "an equivalent adiabatic process". Unfortunately, the interpretation of detailed component investigations in terms of these entropy-rise

efficiencies are not always consistent with the usage in cycle analyses, and the performance figures obtained may be quite far removed from what actually is implied in experiments, or component analyses.

In the exhaust nozzle, the large part of the flow is adiabatic and generally shock free. Irreversible processes are either due to boundary layers, which are restricted to a relatively small part of the flow, or due to chemical nonequilibrium which is best understood from a thermodynamic viewpoint. Hence, thermodynamic measures of exhaust nozzle losses are convenient. However, appropriate definitions of mean flow quantities are still troublesome.

In the simplified model of the engine, a fixed geometry engine with a constant area combustor and an exhaust nozzle exit area equal to the frontal area of the engine is taken as a reference. In the sense that most engine designs will have a fixed geometry, themodel is somewhat more realistic than rubber engines where the pressure or enthalpy ratios are fixed. Let us consider an idealized supersonic combustion ramjet as sketched in Figure 3.1. By convention, ramjet internal thrust is defined by the net change in momentum of the fluid passing through the engine, less the ambient pressure area terms:

$$F_{int} = \dot{m}_6 V_6 - \dot{m}_0 V_0 + (P_6 - P_0) A_6 \qquad (3.1a)$$

In practice, especially with the exotic nozzle configurations, the exit velocity V_6, pressure P_6, and even the area A_6 can be difficult to define in a manner suitable for engine performance calculations. It is convenient therefore to define a mass flow average specific impulse

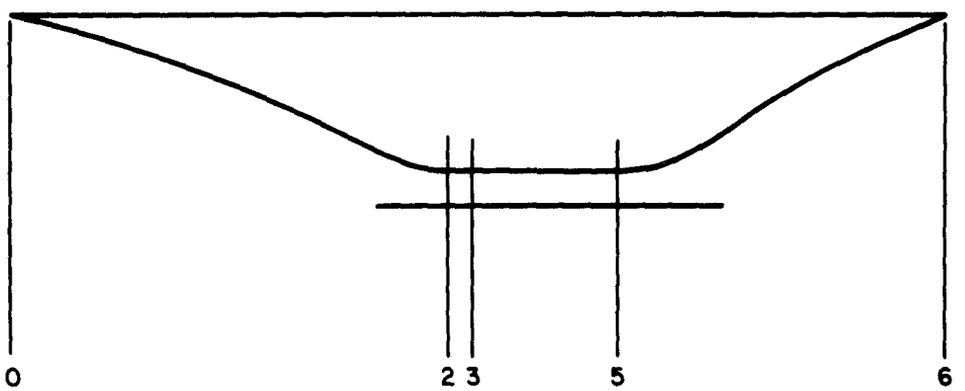

ENGINE STATION LOCATIONS

0	FREESTREAM
2	DIFFUSER EXIT
3	FUEL INJECTION
5	COMBUSTOR EXIT
6	NOZZLE EXIT

FIGURE 3.1
SCHEMATIC SCRAMJET

function which would be a direct measure of stream thrust per unit of mass flow. We shall designate the specific impulse function by the symbol j and define it as an integral quantity averaged to take into account nonuniform flow:

$$j \equiv \frac{1}{\dot{m}} \int_0^{\dot{m}} V_x \, d\mu + \frac{1}{\dot{m}} \int_0^{A} P \cos\alpha \, dS \tag{3.2}$$

where V_x is the axial component of velocity and α is the angle of the normal to the elemental control surface with respect to the axis. In subsequent discussion it will be assumed that the velocity vector is substantially aligned with the axis, and that the projected elemental area dA designates Cos α dS. Equation (3.1a) is then written in the more general form:

$$F_{int} = \dot{m}_6 j_6 - \dot{m}_o j_o + P_o(A_o - A_6) \tag{3.1b}$$

where A_6 is defined as the projected area of the nozzle exit in a plane normal to the axis, and A_o is the capture area at free stream conditions of the air which passes through the engine. The fuel to air ratio will be symbolized by f, so the net fuel specific impulse would be

$$I_{sf} \equiv \frac{F_{int}}{\dot{m}_o f} = \frac{1+f}{f} j_6 - \frac{1}{f} j_o + \frac{V_o}{f \gamma M_o^2}\left(1 - \frac{A_6}{A_o}\right) \tag{3.3}$$

We shall modify the Eq. (3.3) so that ratios of the j functions across the inlet, combustor, and exhaust nozzle are called out:

$$I_{sf} = \frac{j_o}{f}\left[(1+f)\frac{j_6}{j_{6i}} \cdot \frac{j_{6i}}{j_3} \cdot \frac{j_3}{j_2} \cdot \frac{j_2}{j_o} - 1\right] + \frac{V_o}{f \gamma M_o^2}\left(1 - \frac{A_6}{A_o}\right) \tag{3.4}$$

The various impulse functions are defined below:

j_6 mass flow average impulse function at the nozzle exit

j_{6i} impulse function at the nozzle exit for isentropic expansion over the same area ratio.

j_5 mass flow average impulse function at the combustor exit

j_2 mass flow average impulse function for the air stream at the combustor entrance

j_0 free stream impulse function

The breakdown of the impulse function in this manner enables one to evaluate the contribution of each component of the engine to the development of the net thrust. In the particular case where the free stream capture to exhaust nozzle area ratio is 1.0, then the contribution of the last term of Eq. (3.4) is zero.

The net thrust of an engine can be computed by adding and subtracting the various forces which are acting on the captured air stream and then summing up to obtain the net gain or loss in the impulse function. This process is illustrated for flight velocities of 8, 16 and 26 thousand feet per second using examples computed using conventional efficiency parameters. The results are given in Figure 3.2. The impulse function based on the fuel mass flow is plotted against arbitrary engine station points corresponding to Figure 3.1. From station 0 to 2, the drop in the impulse function from

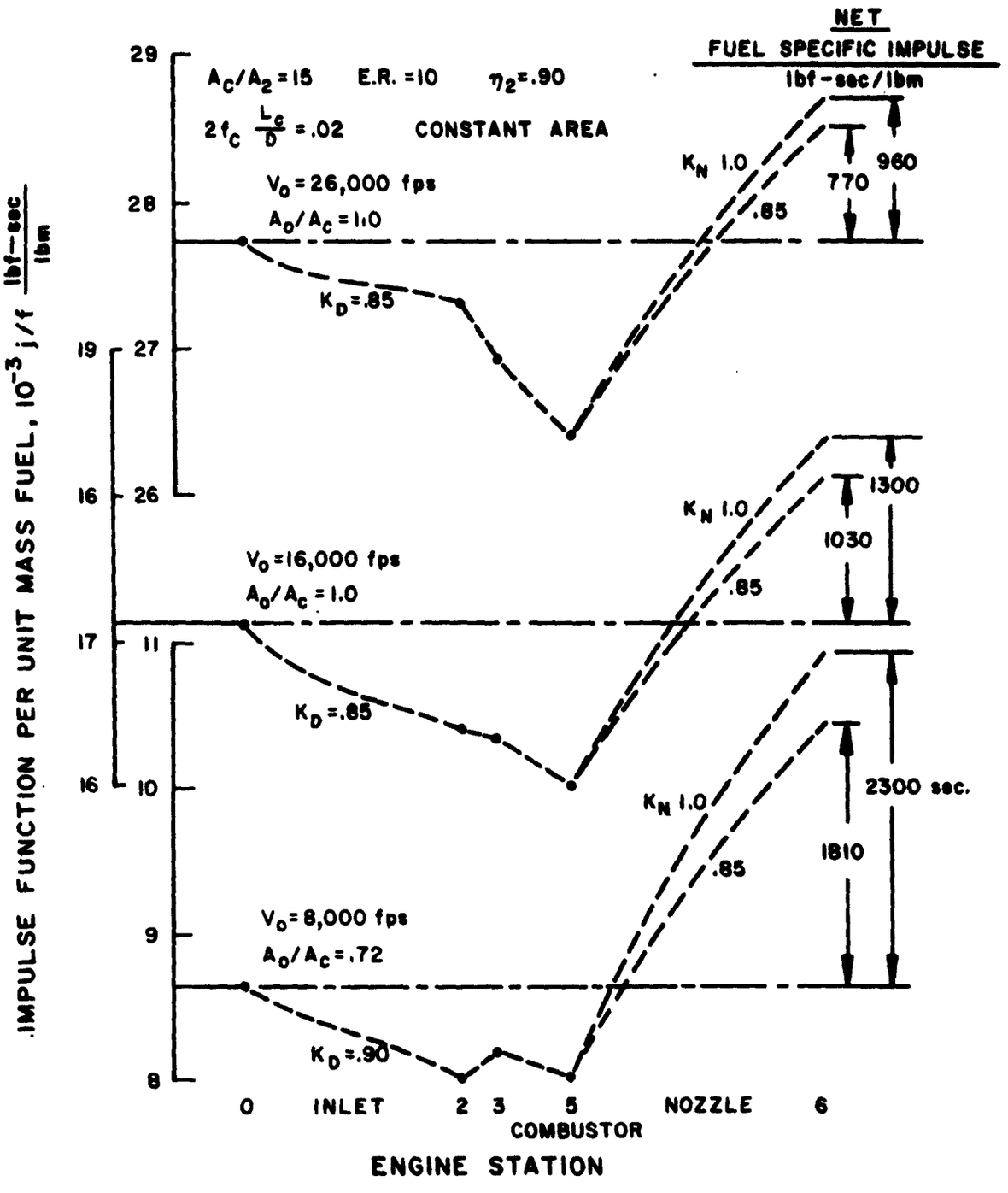

FIGURE 3.2

IMPULSE FUNCTION AT VARIOUS ENGINE STATIONS

the free stream value is due to the inlet compression process. From station 2 to 3, the fuel injection momentum and strut losses are included. The change in the value of the impulse function from station 3 to 5 is attributed to friction alone since a constant area combustor was assumed. The expansion in the exhaust nozzle occurs between stations 5 and 6. The difference between the fuel-flow-based free stream impulse, j_o/f, and the final value at the end of the exhaust nozzle, $(1 + f)j_6/f$, is the net fuel specific impulse. The impulses were computed for two values of the nozzle efficiency parameter K_N. The results plotted in the form of Figure 3.2 are very revealing. One can immediately discern the effect of combustion friction losses, and the relative importance of the inlet, fuel injector, combustor, and exhaust nozzle.

Despite the large differences in the absolute magnitude of the impulse functions, the relative importance seems to be the same for each component at all speeds.

3.4 INLET EFFICIENCY PARAMETERS

Scramjet cycle analyses usually start with some arbitrarily defined inlet efficiency based on thermodynamics. The most commonly used ones (Refs. 1, 2, 3, and 4) are kinetic energy conversion efficiency K_D, the kinetic energy efficiency η_{KE}, the pressure recovery efficiency η_P, and the total pressure ratio P_{t2}/P_{t0}. These efficiencies can all be related to the entropy rise associated

with the shock and friction losses in the inlet. In cases where the air can be assumed to be in thermal equilibrium, the relations are best illustrated on a Mollier chart, as shown in Figure 3.3. The initial conditions are at (h_o, s_o) where the ambient pressure is P_o and total enthalpy is h_{to}. The state at the diffuser exit is (h_2, s_2) where the pressure is P_2 and the total enthalpy is h_{t2}. The difference in total enthalpy is attributed to heat loss in the inlet stream. Various hypothetical state conditions are introduced in order to obtain reference states on which to base an efficiency measure. These various thermodynamic efficiencies, defined in terms of the quantities illustrated in Figure 3.3, are

$$\eta_{KE} = \frac{h_{to} - h'_{oi}}{h_{to} - h_o} \tag{3.5a}$$

$$K_D = \frac{h'_2 - h'_{oi}}{h'_2 - h_o} \tag{3.5b}$$

$$\eta_P = \frac{P_2}{P_{2i}} \tag{3.5c}$$

Some variants of these definitions are used, especially where there is a heat loss to be considered, but those listed above are the most common.

3.5 INLET INTERNAL DRAG COEFFICIENT

Inlet performance can also be expressed in terms of aerodynamic coefficients. Among these are the internal drag coefficient of the inlet, and the stream impulse ratio j_2/j_o for a fixed area ratio.

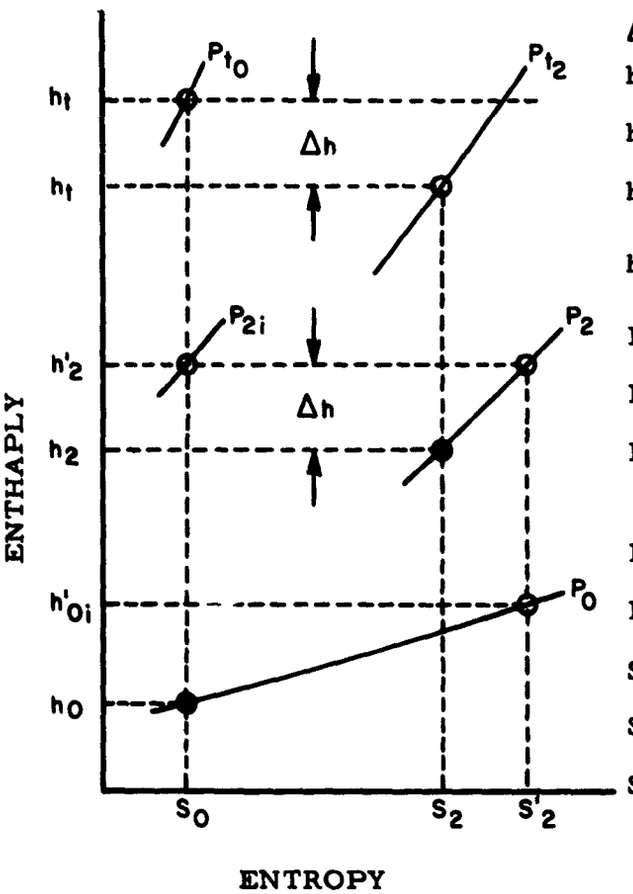

h_o	free stream enthalpy
h_2	diffuser exit enthalpy
Δh	heat loss in diffuser
h_{to}	free stream total enthalpy
h_{t2}	diffuser exit total enthalpy
h'_2	diffuser exit enthalpy with heat loss restored
h'_{oi}	enthalpy for isentropic expansion from h'_2, P_2 to P_o
P_o	free stream static pressure
P_2	diffuser exit static pressure
P_{2i}	diffuser exit static pressure for isentropic adiabatic compression
P_{to}	free stream total pressure
P_{t2}	diffuser exit total pressure
S_o	free stream entropy
S_2	diffuser exit entropy
S'_2	diffuser exit entropy for heat loss restored at diffuser exit pressure

● Actual State Points

○ Hypothetical State Points

FIGURE 3.3
SCHEMATIC MOLLIER CHART

If the drag force of the inlet is measured, then an internal drag coefficient can be defined as

$$C_D = \frac{D_s - D_A}{q_o A_o} \tag{3.6}$$

where A_o is the free stream capture area, D_s is the drag force on the internal wetted surface and D_a is the additive drag due to spillage around the cowl. The ratio of the stream impulse function j_2/j_o is then simply related to C_D by

$$\frac{j_2}{j_o} = 1 - \frac{\gamma M_o^2}{1+\gamma M_o^2}\left[\frac{C_D}{2} + \frac{1}{\gamma M_o^2}\left(1 - \frac{A_2}{A_o}\right)\right] . \tag{3.7}$$

Either C_D or the j_2/j_o ratio can be used as measures of inlet performance. Note that j_2 enters directly into the combustor momentum balance, hence pressure, velocity, temperature and density are not required except to aid in evaluating combustor friction, wall pressures, and heat loss. A plot of j_2/j_o calculated by Eq. (3.7) is given in Figure 3.4 for various values of C_D, and Mach numbers. The influence of the area ratio A_2/A_o is so small that it is indetectable on this plot.

The relation between C_D and the kinetic energy conversion efficiency K_D are given in Figures 3.5, 3.6, 3.7, and 3.8 for given values of capture area ratio A_o/A_2 and flight Mach number. These K_D values apply only to cases of adiabatic flow, and uniform combustor inlet conditions. Conversion to other efficiency measures can be obtained from plots given in Refs. 1 and 3. For the one case reported so far where Scramjet inlet drag has been measured

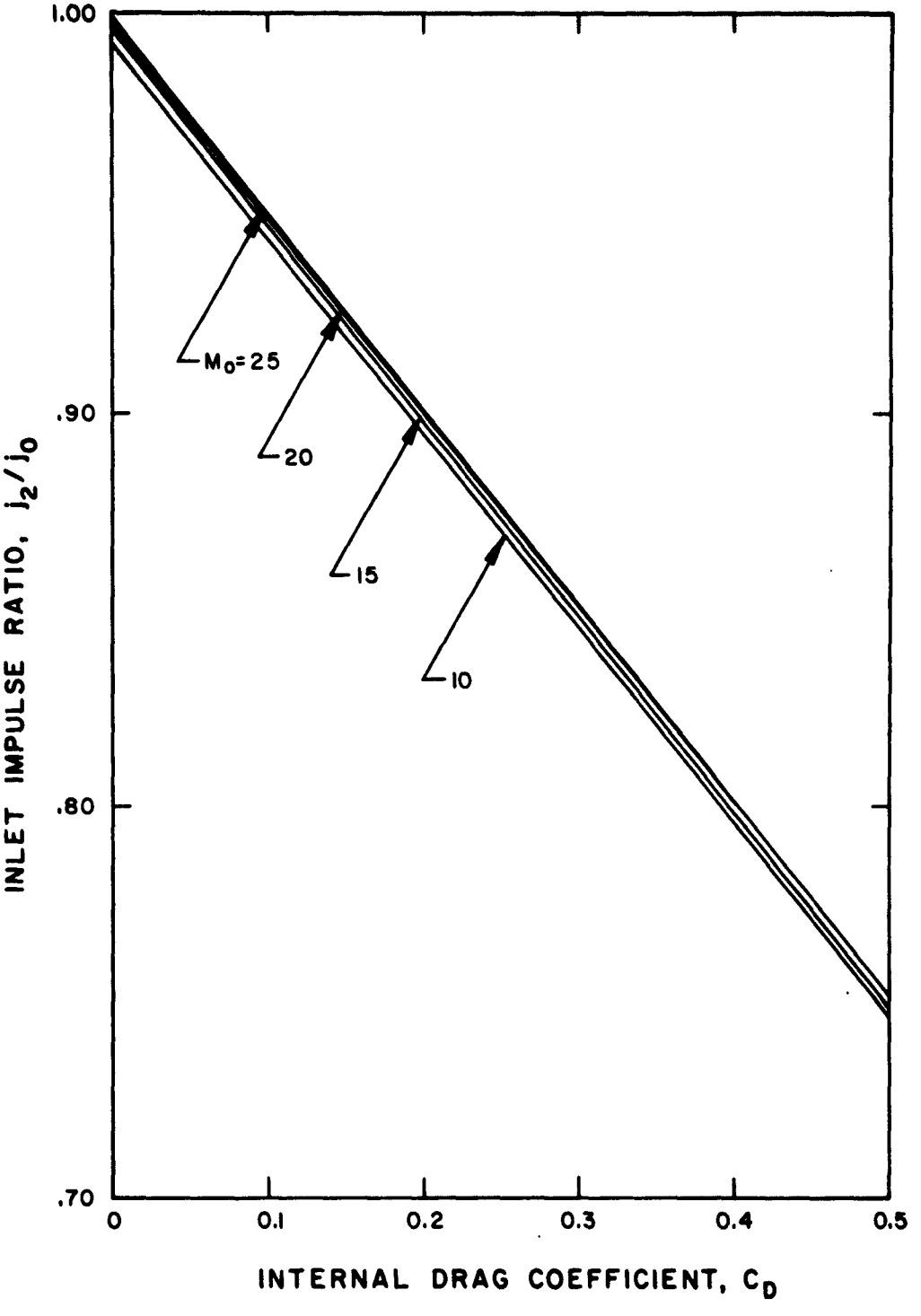

FIGURE 3.4
INLET PERFORMANCE- INLET IMPULSE RATIO VS INTERNAL DRAG COEFFICIENT

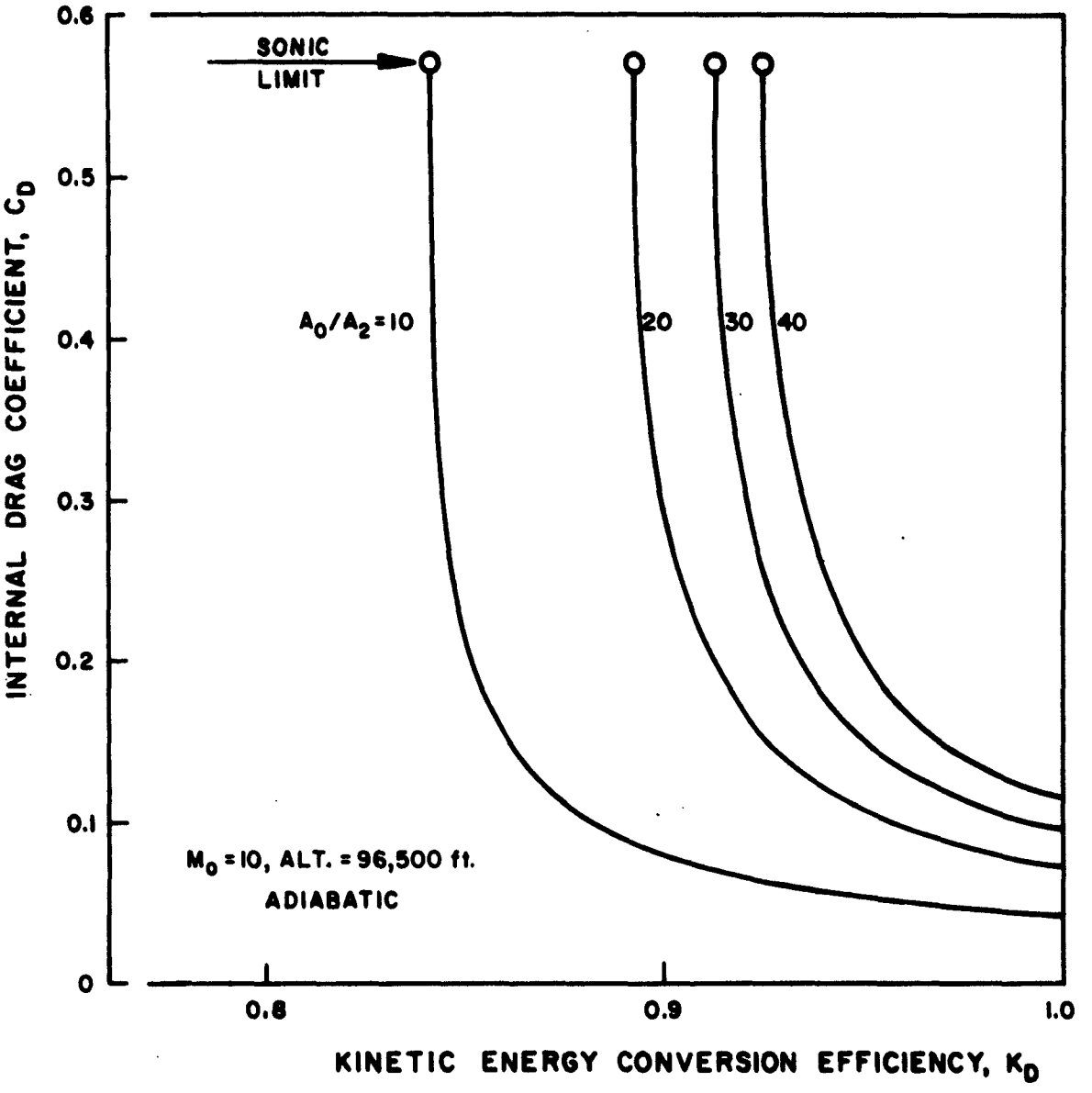

FIGURE 3.5
INLET INTERNAL DRAG COEFFICIENT VARIATION WITH INLET KINETIC ENERGY CONVERSION EFFICIENCY

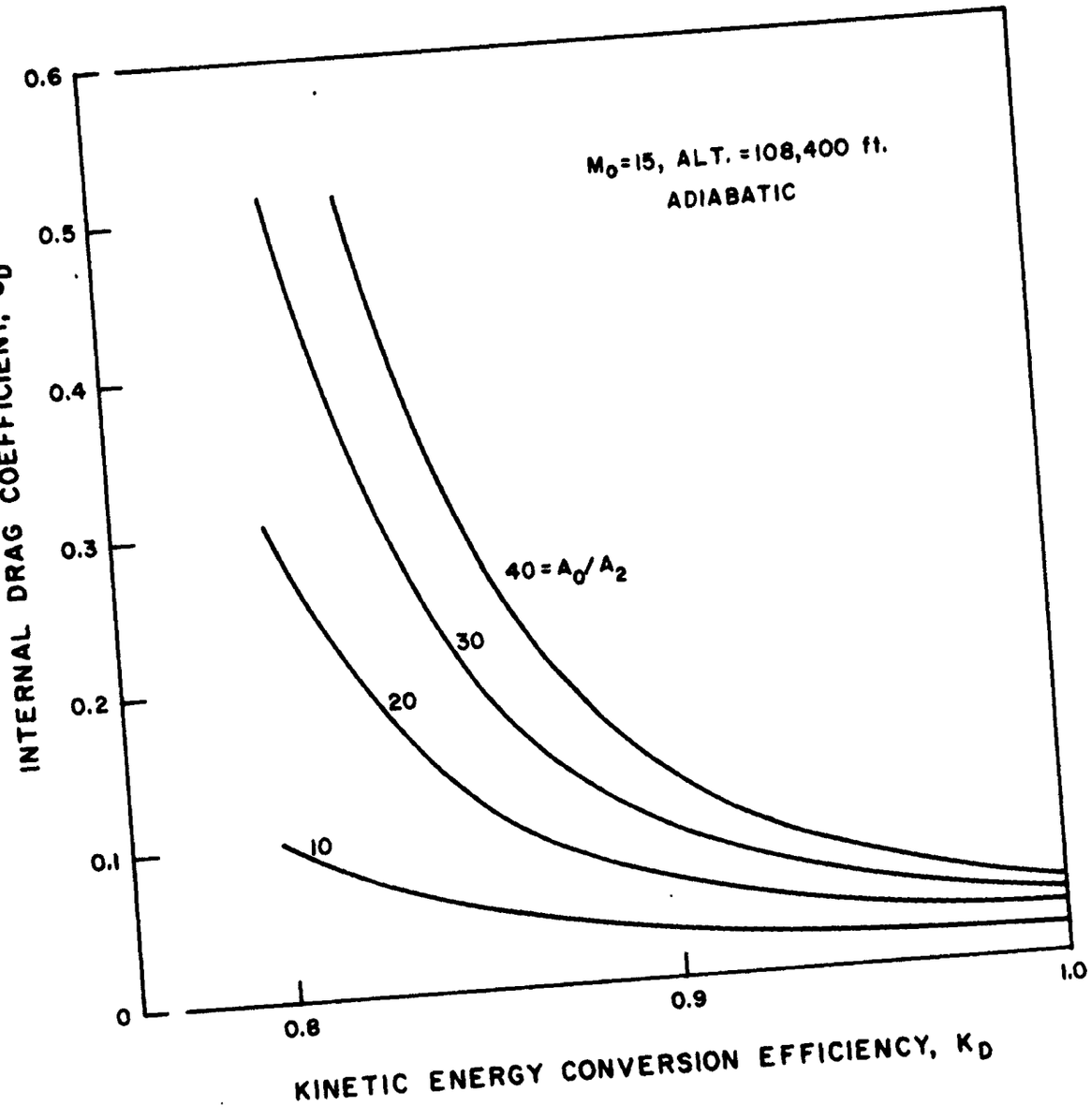

FIGURE 3.6
INLET INTERNAL DRAG COEFFICIENT VARIATION WITH INLET KINETIC ENERGY CONVERSION EFFICIENCY

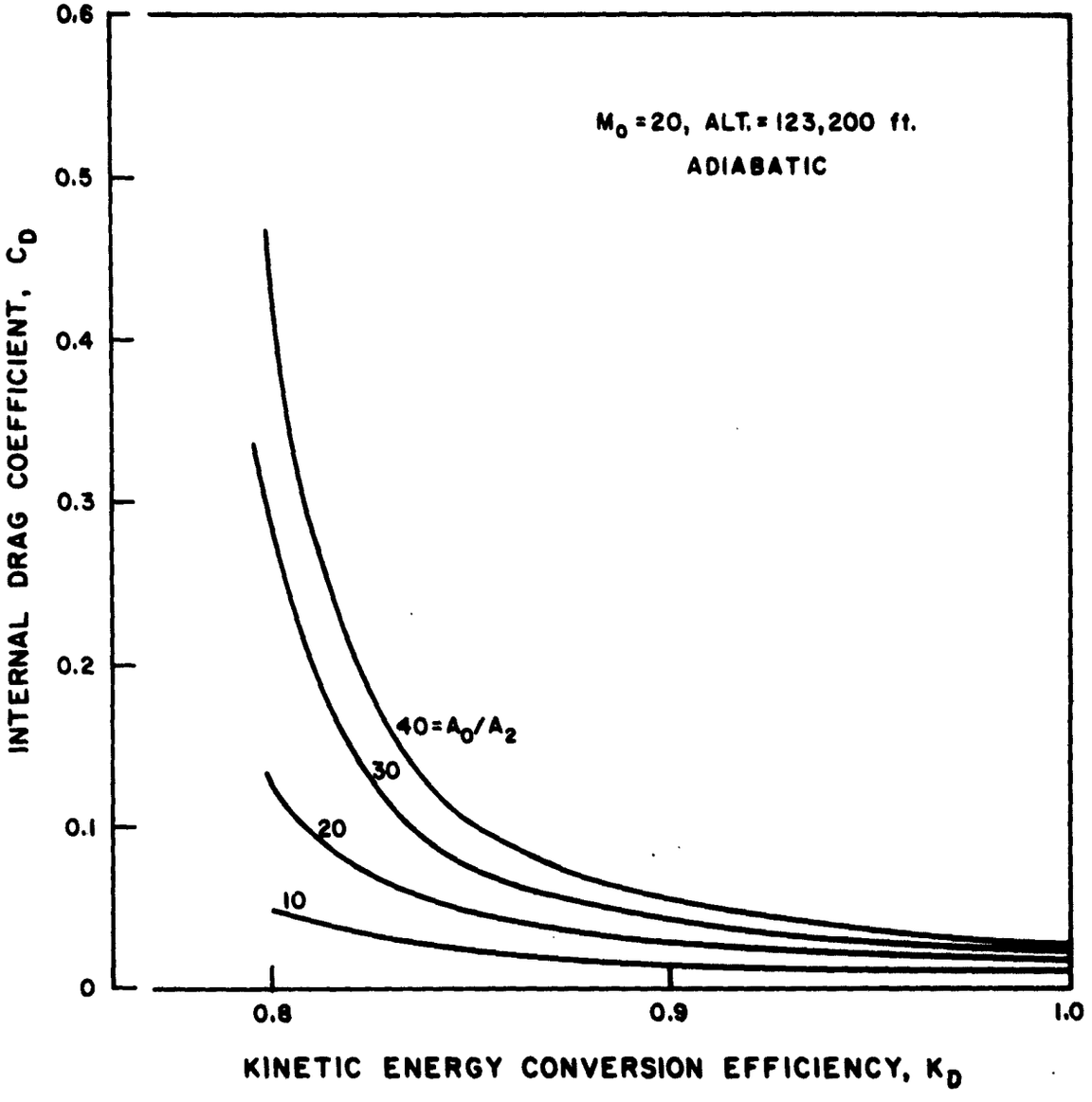

FIGURE 3.7
INLET INTERNAL DRAG COEFFICIENT VARIATION WITH INLET KINETIC ENERGY CONVERSION EFFICIENCY

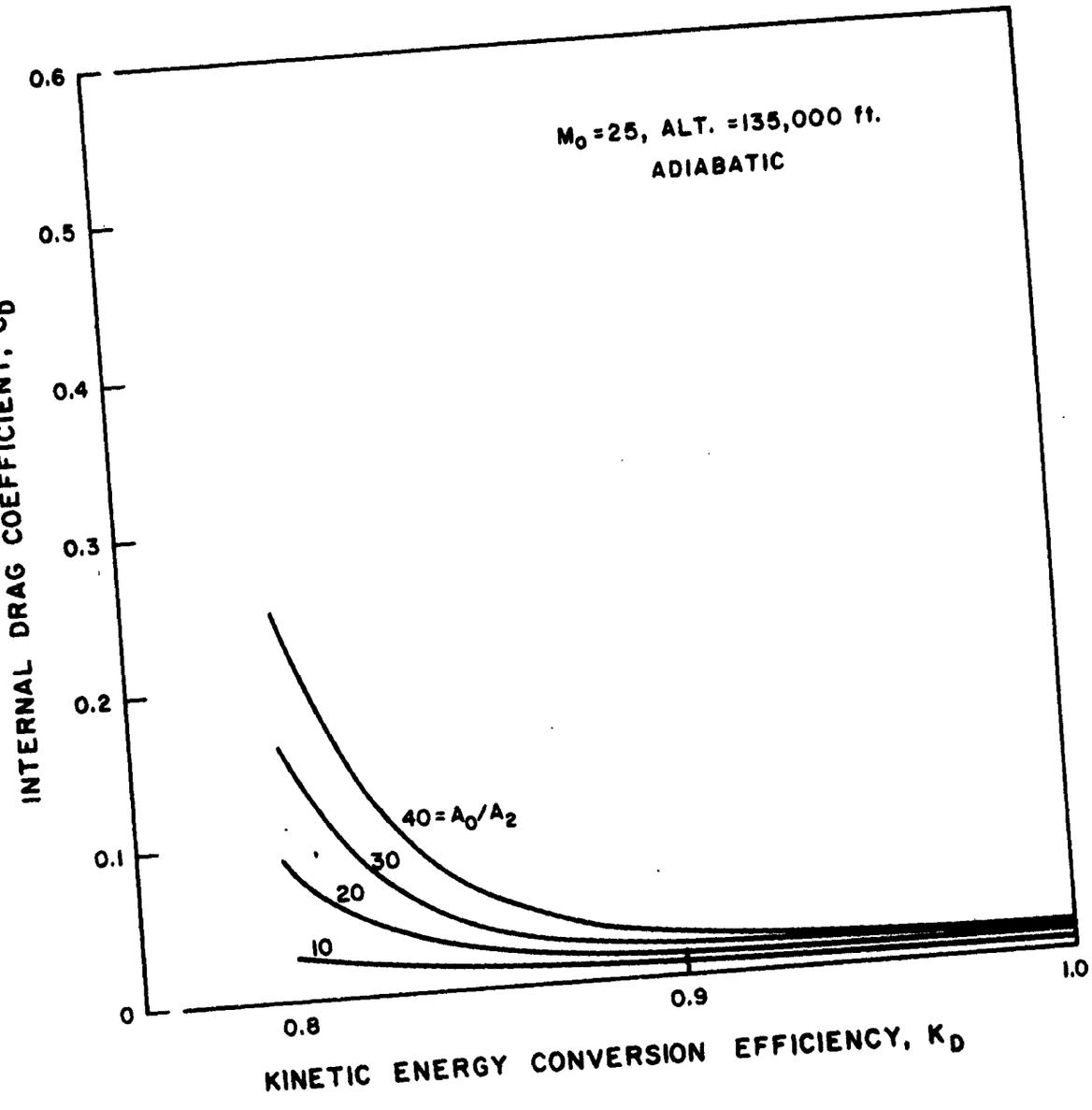

FIGURE 3.8
INLET INTERNAL DRAG COEFFICIENT VARIATION WITH INLET KINETIC ENERGY CONVERSION EFFICIENCY

experimentally (Refs. 2, 11), the experimental C_D as a function of area ratio are given in Figure 3.9.

The experimentally measured internal drag coefficient C_D implicitly contains terms for the drag due to the inviscid pressure, the induced pressure due to boundary layer displacement, and the wall friction. Corrections of experimental data on model inlets to full scale inlets can then be made by applying corrections to each of these terms. In this respect, the hypersonic simulation technique used by the General Electric Company (Ref. 1) is probably the best method of obtaining applicable data short of full simulation testing. From hypersonic scaling relations (Ref. 10), the contribution of the inviscid pressure field and the induced pressure to the overall internal drag coefficient C_D are the same for the model as for the full scale provided that the similarity parameters (Md/L), $M^3 \sqrt{C} / \sqrt{R}$, h_w/h_e and $M(t/L)^3$ are held constant. There is however a correction for the part of the drag coefficient due to viscous shear. The viscous shear losses will increase approximately as the Mach number. Hence simulated inlet drag coefficient data obtained at Mach 16 will be about 3% to 16% lower than if the inlet were tested at Mach 25. This correction is probably negligible in the first approximation but should be included if the test data on drag coefficients are sufficiently reliable. The same correction should be applied to the measured pressure recovery coefficient η_P although the percent correction would vary with the actual value of η_P.

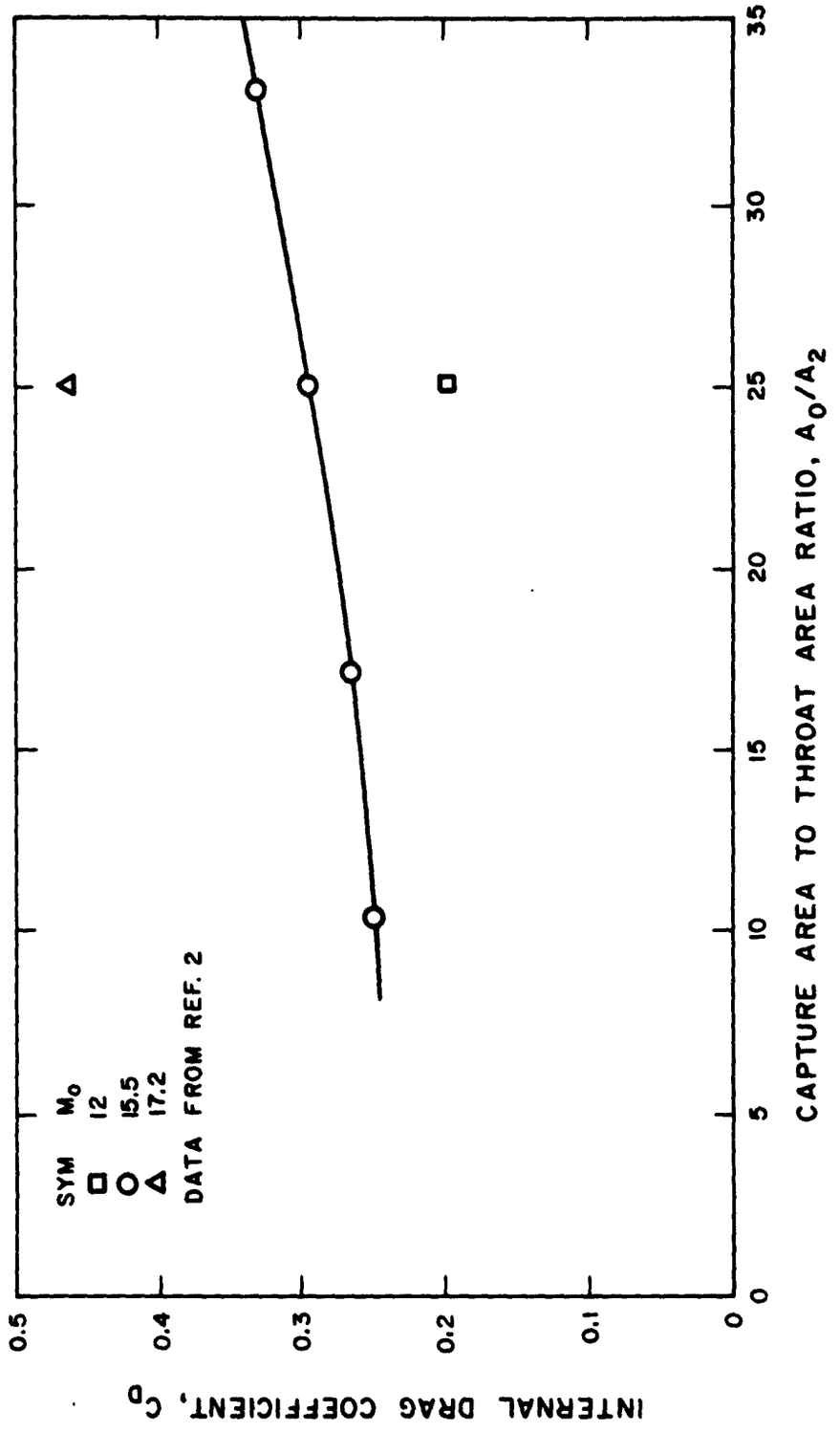

FIGURE 3.9
EXPERIMENTAL INLET DRAG COEFFICIENT

The substitution of a gas with a different specific heat ratio such as helium would not maintain similarity. The specific heat ratio is a similarity parameter in itself (Ref. 10), hence theory requires that this parameter be the same to maintain correspondence.

The General Applied Science Laboratory has used the principles of hypersonic similitude in nozzle flow (Ref. 3). In one test setup, the geometry and specific heat ratio are simulated while an entirely different test is required to maintain chemical similarity.

Heat loss to the walls of the inlet would be expected to have a relatively small effect on the drag coefficient C_D. However it can have a large effect on the ave rage static pressure measured at the diffuser exit. Using experimentally determined static pressures at the exit station can lead to gross errors in the reported efficiency parameters unless the heat losses are measured and inlet nonuniformity taken into account.

Theoretical performance estimates for Scramjets along projected trajectories have been reported in Refs. 1 and 2. The inlet performance given in these parametric studies has been interpreted in terms of fuel specific impulse as a function of the inlet internal drag coefficient as shown in Figure 3.10. The linear decrease of I_{sf} with increase in C_D may be noted. For comparison experimental inlet drag values are about 0.25 to 0.33 for approximately the same Mach number and range of area ratios. The discrepancy between the required and experimental inlet drags are obvious.

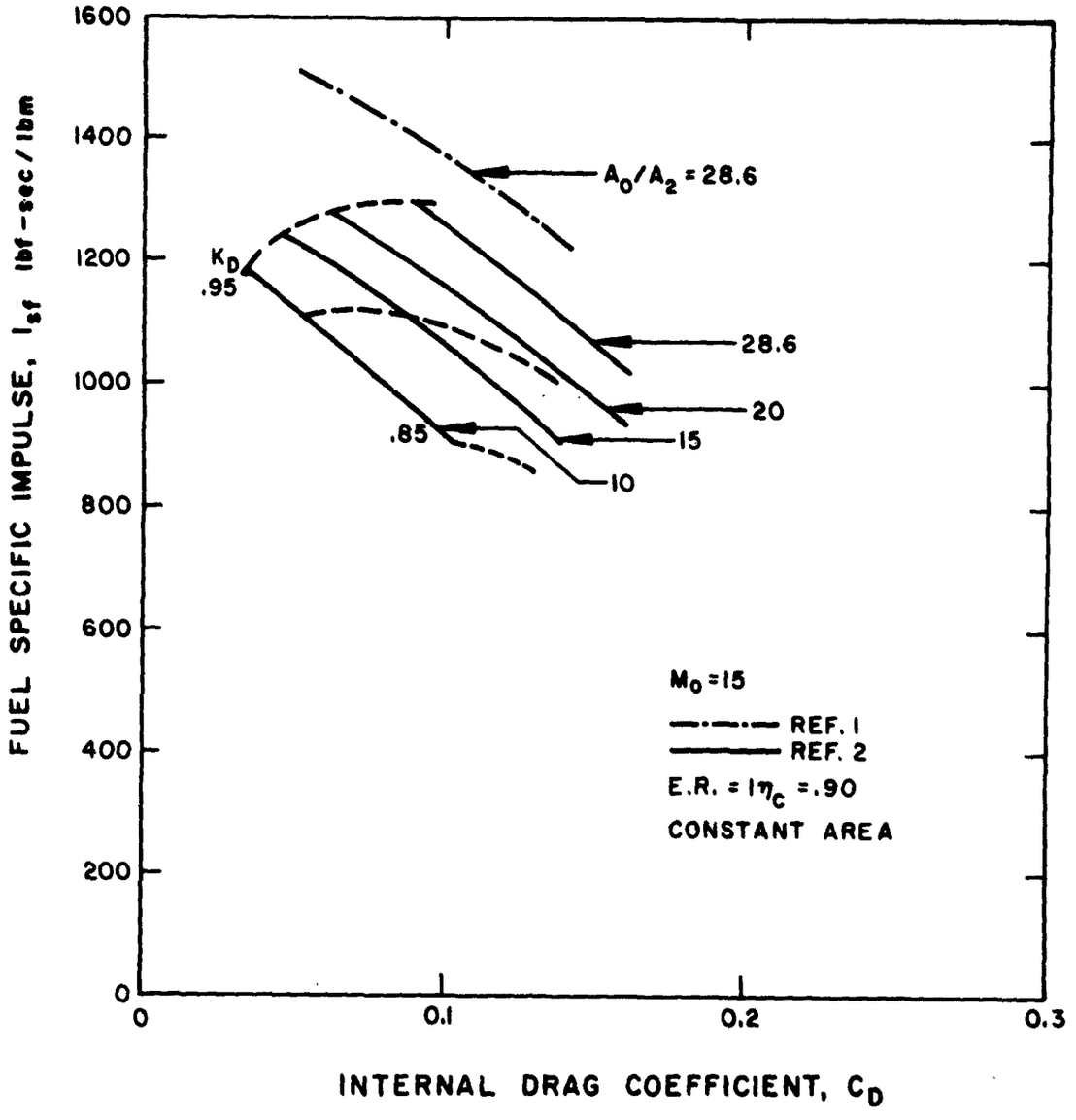

FIGURE 3.10
EFFECT OF INLET INTERNAL DRAG COEFFICIENT ON FUEL SPECIFIC IMPULSE

3.6 NONUNIFORM FLOW AT THE DIFFUSER EXIT

A number of studies purporting to include the effect of nonuniform flow at the diffuser exit on performance have been made (Refs. 1, 5, 6). The study in Ref. 6 considers only the boundary layer displacement and momentum defect as a source of flow distortion. As pointed out in Ref. 4 this is probably the lower limit of distortion effects on the mean static pressure ratio. The flow distortions considered in Ref. 1 assume again that boundary layers are the main disturbance. Both the analyses in Refs. 1 and 6 have in common the assumption that the flow distortions are essentially carried through to the ends of the combustor relatively undisturbed by the mixing and combustion of the fuel. Detailed studies (Ref. 7), however, indicate that the effects of combustor entrance boundary layer do not persist very far into the combustor. The type of nonuniform flow obtained at the combustor exit is much more a characteristic of the combustor itself, and not of the initial distortions. This conclusion will be valid even if the major cause of inlet nonuniformity is due to the inlet shock structure (Ref. 4). It follows therefore that to a fair approximation, there is no need to know the combustor entrance flow nonuniformities. Only the mass flow average impulse j_2, total enthalpy h_{t2}, and the mass flow per unit area need be determined at the combustor inlet. In order to make this point clearer, consider an inlet which has a fixed drag coefficient, C_D as defined in Eq. (3.6) and a fixed area ratio. Then j_2 will be fixed.

There are a number of different designs which would give the same value of j_2 but due to the different configurations, the profiles of velocity would be different. If these inlets were attached to the same combustor, then it can be assumed for not too drastic distortions that the flow coming out of the combustor will have essentially the same profile. The hypothesis of independence of the combustor exit flow profile from the inlet flow profile should be more valid with highly efficient mixing and large fuel flow rates. This does not imply that inlet flow distortions are not important since there may be local interaction of the flow with the fuel injection which can cause separation and result in incomplete mixing. It does mean however that with fairly efficient inlets matched to fairly efficient combustors, changes in the inlet displacement thickness or similar nonuniformity parameters should have negligible effect on the over-all engine performance.

If the viewpoint of the above argument is accepted, it becomes obvious that the major purpose of any measure of the Scramjet inlet performance should be that of producing the correct value of the impulse function at the diffuser exit. Most measures of inlet diffusion efficiency (e.g. η_{KE}, K_D, η_P, or P_{t2}/P_{to}) are defined using the pressure ratio and enthalpy ratio. It has been shown however (Ref. 4) that of all the mean properties one can find at the diffuser exit, the pressure is the one most sensitive to flow distortion. Hence, the use of a pressure ratio in the definition of an efficiency must necessarily be accompanied by a specification of an inlet nonuniformity parameter. Otherwise the use of this efficiency value

becomes subject to gross errors.

To illustrate this point, we use an analysis due to Ref. 8 for a Mach 16 inlet with an area ratio A_o/A_2 of 25. In Figure 3.11a the impulse ratio j_2/j_o is plotted as a function of the internal drag coefficient C_D. Figure 3.11b is taken directly from Ref. 8 which shows the relation between the displacement thickness Δ^*/A_2, the pressure recovery coefficient η_P, and drag coefficient. If we compare two inlets with the same area ratio and drag coefficient but with different displacement thickness, different values of the pressure recovery η_P would be computed (see dashed lined in Figure 3.11) yet the engine performance of these two would be exactly the same, since the same value of j_2/j_o would be obtained.

3.7 COMBUSTOR FRICTION

The impulse at the diffuser exit, j_2, enters directly into the momentum balance around the combustion chamber. The equation for the combustion chamber momentum balance in terms of the impulse functions is

$$j_s = \frac{j_2 + f j_f}{1+f} - \int_0^{L_c} f_c \frac{q_c S_c}{\dot{m}} dL + \int_0^{L_c} P \frac{dA}{dL} dL \qquad (3.8)$$

where j_f is the impulse of the fuel in the axial direction evaluated at the combustor control surface; f_c, q_c, L_c and S_c are the combustor friction factor, dynamic pressure, length, and wetted perimeter, respectively, and the last term of Eq.(3.8) is the wall pressure integral in the combustor. The equation for energy conservation, assuming that the radiative heat loss (as opposed to regenerated heat loss)

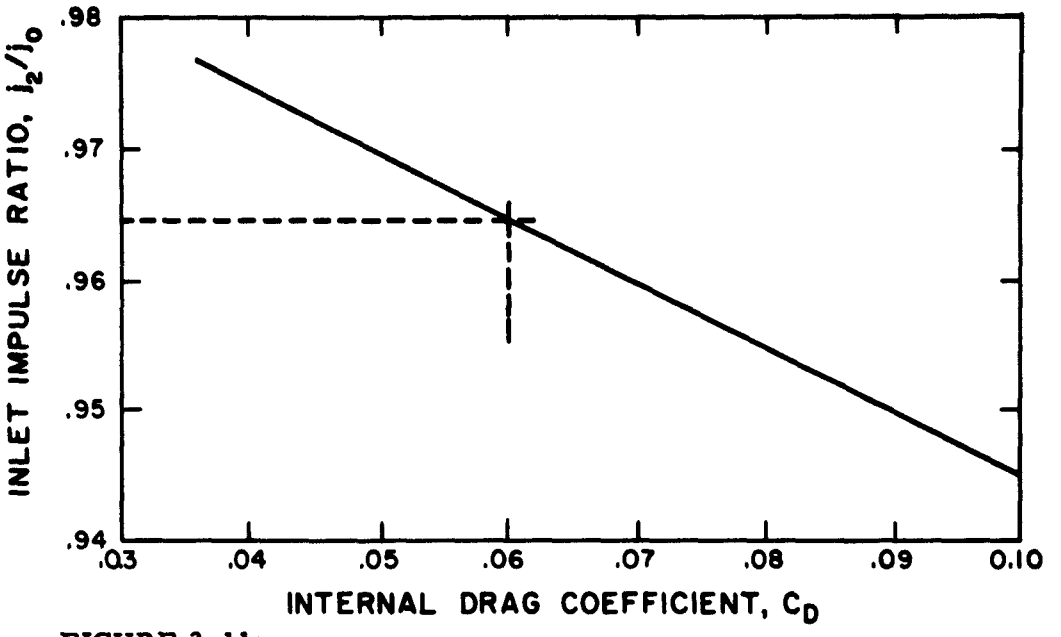

FIGURE 3.11a

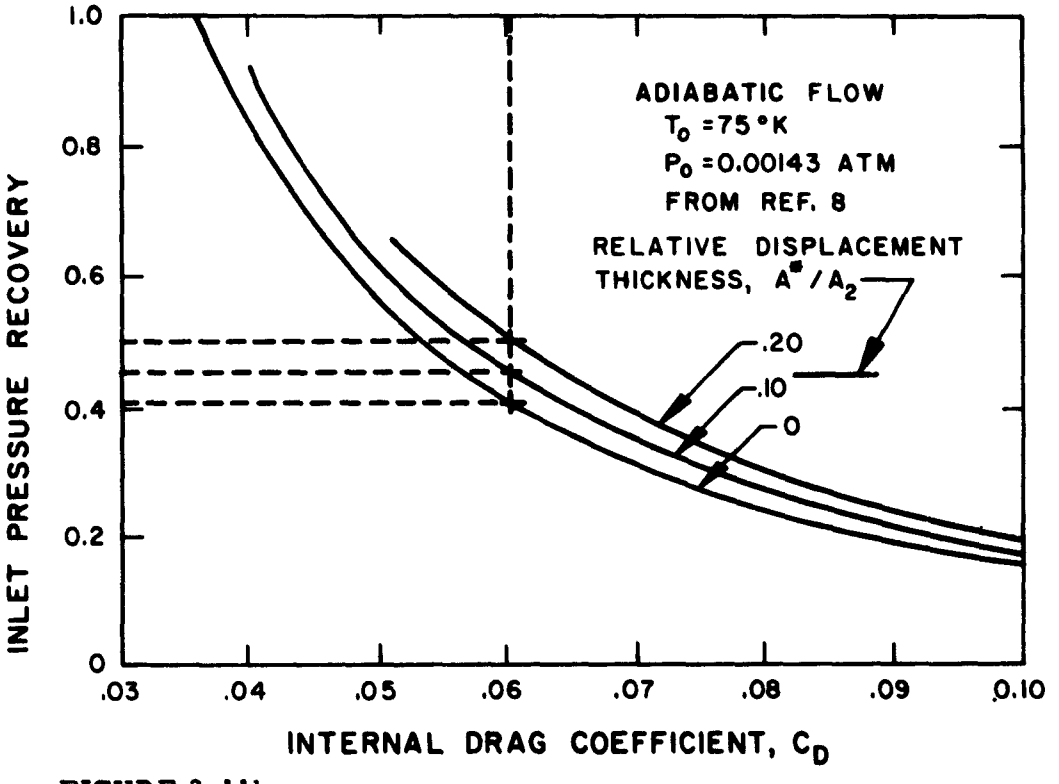

FIGURE 3.11b

FIGURE 3.11

NON-UNIFORM FLOW EFFECTS - INLET IMPULSE RATIO AND PRESSURE RECOVERY $M_o = 16$, $A_0/A_2 = 25$

is known, is

$$h_{t_5} = \frac{h_{t_2} + f h_f + \eta_c f' \lambda^\circ_f}{1+f} - \Delta h_c \qquad (3.9)$$

where h_f is the sensible enthalpy of the fuel before regenerative cooling, $\eta_c f' \lambda^\circ_f$ is the effective heat release, and Δh_c is the permanent heat loss within the combustor. A seeming anamoly exists in evaluating j_f at the combustor control surface where the fuel temperature is at its maximum and evaluating the energy balance with the fuel at the entrance temperature. This is resolved when one considers that the increase in fuel temperature occurs only due to convective cooling and must be accompanied by friction losses. With complete regenerative cooling, the increase in fuel impulse j_f due to combustion chamber cooling generally will not completely balance the loss in combustor exit impulse j_5 due to friction.

From an approximate evaluation of the combustor friction in a constant area supersonic duct, the wall friction term can be put proportional to the impulse function at the combustor exit

$$\int_0^{L_c} f_c \frac{q_c S_c}{\dot{m}} dL_c \cong 2 \bar{f}_c \frac{L_c}{D} j_5 \qquad (3.10)$$

where $\bar{f}_c$ is the mean combustor friction factor and D is the hydraulic diameter of the duct. Thus Eq.(3.8), for a constant area duct, becomes

$$\frac{j_5}{j_2} = \frac{1 + f(j_f/j_2)}{(1+f)(1+2\bar{f}_c L_c/D)} \qquad (3.11)$$

The ratio of the fuel impulse to the air impulse at the combustor entrance j_f/j_2 can be taken as approximately equal to the velocity ratio if both are sufficiently supersonic ($M_f > 2$, $M_2 > 2$). For typical conditions, the ratio j_f/j_2 ranges from 2 at Mach 8 to about 1/2 at Mach 25 (Ref. 1 and 2) when the fuel temperature is held at 2000° F. However, if fuel temperature is allowed to vary with combustor heat loss, then j_f will increase approximately as the square root of the total regenerative heat loss. The net effect of regenerative cooling is that the ratio j_5/j_2 expressed in Eq. (3.11) will decrease below the value obtained with no regeneration.

3.8 COMBUSTOR EXIT AND EXHAUST EXPANSION

The main purpose of the combustion duct is to mix the fuel and air and to obtain most of the chemical reactions of combustion. On the other hand the main purpose of the exhaust nozzle is to increase the momentum of the flowing stream as much as possible. The combustor losses in momentum discussed previously are a perturbing factor on the operation of the combustor while the major processes of the combustor are considered as perturbations in the operation of the exhaust nozzle. Hence it is convenient to separate the considerations of combustor and exhaust nozzle, even though the same physical and thermodynamic processes are operative. The dividing control surface is not always clearcut, but it will be assumed that such a division can be made.

In most analyses of the exhaust nozzle it is assumed that

heat release due to residual combustion is equal to that of an equivalent equilibrium gas down to a freezing point, and also that no further mixing occurs within the nozzle. The combustion is, therefore, charged with all losses in heat release due to incomplete reaction and mixing. If the combustor exit velocity, enthalpy, pressure, and mixture ratio were known for each stream tube, it is a fairly straightforward, though tedious, procedure to use a rotational method of characteristics to evaluate the inviscid flow field of the nozzle. However, these procedures are restricted to carefully specified combustor-nozzle combinations. Therefore, to obtain more general analyses, a means of obtaining useful efficiency parameters is desirable. It has often been stated (Refs. 1, 2, 5, 6) that it is not possible to choose mean values of temperature, pressure, density, and velocity to satisfy simultaneously the requirements of mass, momentum, area and energy conservation. However, the viewpoint taken at NESCO is that there are mean values which satisfy these requirements provided that one uses properly defined nonuniformity coefficients in the manner of Crocco (Ref. 12). The "ideal" nozzle process is defined in this case as the one-dimensional, isentropic expansion of a uniform, equilibrium combustion gas having the same combustor exit impulse, fuel-to-air ratio, mass flow per unit area, and total enthalpy (after reaction and mixing heat losses are subtracted) over the given area ratio of the nozzle. The equivalent, real expansion process would then have losses due to nozzle friction,

heat loss, nonequilibrium reactions, residual mixing, contouring, and nonuniform entrance conditions. The loss in performance is then usually evaluated as a velocity coefficient, kinetic energy conversion efficiency, gross thrust coefficient, or an impulse efficiency ratio.

The velocity coefficient, C_v, is defined as

$$C_V = \frac{V_6}{V_{6i}} \quad . \tag{3.12}$$

The square of the velocity coefficient is the kinetic energy efficiency for the nozzle. The kinetic energy conversion efficiency, K_N, is defined as

$$K_N = \frac{V_6^2 - V_5^2}{V_{6i}^2 - V_5^2} = \frac{h_5 - h_6}{h_5 - h_{6i}} \quad . \tag{3.13}$$

These kinetic energy parameters suffer the same defect as the analogeous ones in the inlet, namely that mean velocities, pressures, and enthalpys at the combustor exit and nozzle exit must be carefully defined in order to compute the corresponding impulse. More direct measures of the efficiency are the gross thrust ratio

$$\frac{F_6}{F_{6i}} = \frac{\dot{m}_6 j_6 - P_0 A_6}{\dot{m}_6 j_{6i} - P_0 A_6} \tag{3.14}$$

or the related impulse function efficiency

$$C_{Ej} = \frac{j_6}{j_{6i}} \quad . \tag{3.15}$$

These two coefficients can be used directly in the gross thrust equation (Eq. 3.1b) or the impulse equation (Eq. 3.4). The use of

the impulse function efficiency C_{Ej} is to be preferred because internal nozzle losses do not depend upon the ambient pressure. It has been shown in Ref. 1 that the gross thrust ratio F_6/F_{6i} is equal to the velocity coefficient C_V. The relation between C_V and K_D has been discussed in Ref. 3. The relation between C_{Ej} and C_V is presented in Figure 3.12. Objections have been raised to the use of C_V, C_{Ej} and F_6/F_{6i} because the numerical values of these coefficients are very close to unity. Hence 3 to 4 significant figures must be carried in computations. In the case of C_V such objections are valid since the alternative K_N efficiency measure is more sensitive to losses. However in the case of C_{Ej} and F_6/F_{6i}, it is felt that the slight disadvantage of the number of significant figures used in computations is more than outweighed by the advantage that such figures of merit enter directly into the nozzle flow computations, without requiring further evaluation of nebulously defined mean exhaust velocity and pressure. Gas properties enter into performance analyses only in evaluation of well defined one-dimensional uniform isentropic expansion. The reduction of experimental data on nozzle flow becomes considerably easier in this way.

3.9 CONCLUSIONS

1. The study of the Scramjet engine cycle is very much hampered by a cumbersome means of reporting component performance in terms of "an equivalent thermodynamic process efficiency", especially in inlet investigations. The use of drag pressure,

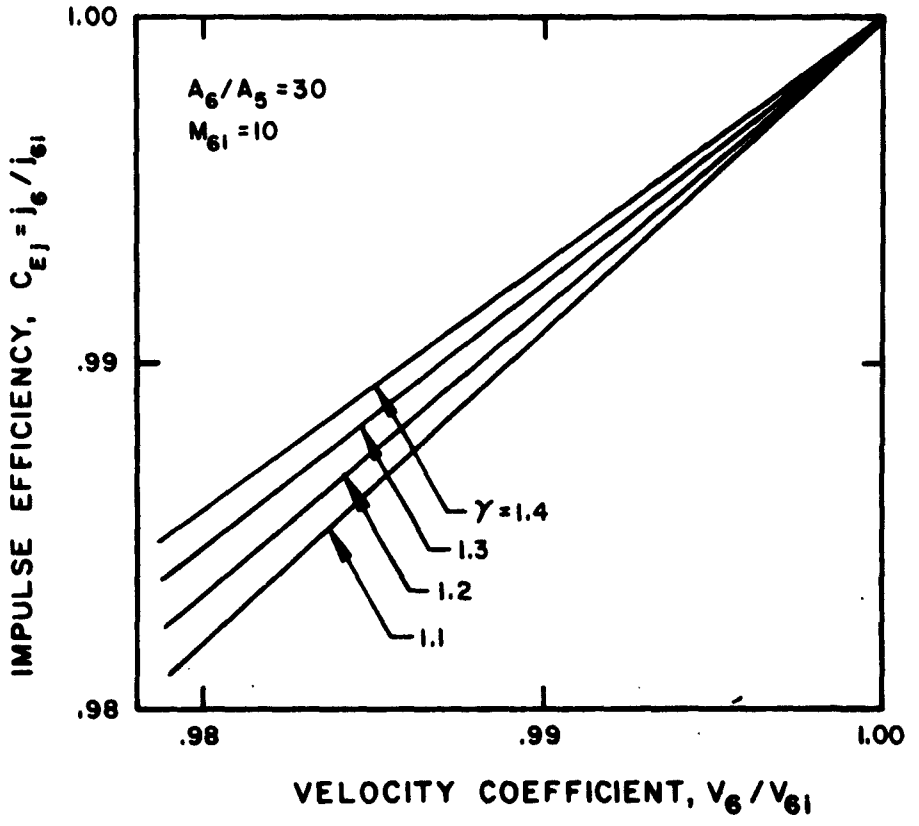

FIGURE 3.12
NOZZLE IMPULSE EFFICIENCY VS VELOCITY COEFFICIENT

and heat loss coefficients would be preferable.

2. The explicit use of the impulse function in the momentum equation leads to considerable clarification of the role of various losses occurring in the Scramjet cycle. In particular, the effect of friction is more easily understood and generalized.

3. Figures of merit for inlet and nozzles based on impulse functions such as the internal drag coefficient of inlets are easier to obtain, use and interpret than ones based on enthalpy or velocities.

4. The adoption of internal drag coefficients as a measure of inlet performance will reduce the present emphasis on the need to evaluate nonuniform profiles at the combustor inlet, as far as cycle analysis is concerned. The need to evaluate flow distortion for its effect on fuel mixing and combustion still exists.

5. Experimental testing of inlet models using the principle of hypersonic similitude will lead to drag coefficient figures differing from scaled inlets only in a relatively minor correction of the friction drag. Such testing should be done with simulation of static enthalpy levels if at all possible.

6. Inlet testing with gases other than air is useful for study of separation, transients, and transition and for proof of

theoretical methods. Direct application of measured drags and pressures obtained during such tests are not consistent with similitude theory.

3.10 RECOMMENDATIONS

1. Scramjet investigation of inlets and exhaust nozzle should report their results in terms of drag coefficients or equivalent measures of impulse change. Reduction of data to kinetic energy efficiency or related thermodynamic measures should be discouraged.

2. Explicit use of impulse functions in cycle analyses would lead to better understanding of performance sensitivity. Since all existing Scramjet cycle analyses are based on the implicit use of the impulse function concept, such a change would lead to simpler and more straightforward computer programs.

3. Experimental results should be reported or interpreted as much as possible in terms of forces acting on control surfaces rather than in terms of the "equivalent" process which lead to the same surface forces.

3.11 REFERENCES

1. "Advanced Air-Breathing Engines (U)," Vol. I-II, APL-TDR-64-21, General Electric Company, Evendale, Ohio, 7 May 1964, SECRET REPORT

2. "Applied Research Investigation of the Supersonic Combustion Ramjet Engine (U)," APL-TDR-63-590, The Marquardt Corp., Van Nuys, California, December 1963 SECRET REPORT

3. "Analytical and Experimental Evaluation of Hypersonic Ramjet (U)," APL-TDR-63-591, General Applied Science Laboratories,

Incorporated, Westbury, Long Island, New York, April 1963 CONFIDENTIAL REPORT

4. "Advanced Air Breathing Engine Study (U)," ASD-TDR-62-1093, National Engineering Science Company, Pasadena, California April 1963, CONFIDENTIAL REPORT

5. F. C. Glaser and T. D. Burnette, "Analysis on Nonuniform Flow in the Scramjet Engine (U)," Report 5986, The Marquardt Corporation, Van Nuys, California, April 1963, CONFIDENTIAL REPORT

6. F. C. Glaser and W. C. Saino, "Analytical Models for Scramjet Engine Analysis in Nonuniform Flows (U)," Report 6032, The Marquardt Corporation, Van Nuys, California, March 1964, CONFIDENTIAL REPORT

7. G. Kleinstein, "On the Mixing of Laminar and Turbulent Axially Symmetric Compressible Flows," PIBAL, Report 756, Polytechnic Institute of Brooklyn, February 1963

8. P. H. Kutschenreuter, Jr., "Force Balance Determination of Inlet Performance," ASD-TDR-63-701, ASD 1963 Science and Engineering Symposium, September 1963

9. "Turbine Ramjet Engine Study (U)," SN-86, National Engineering Science Company, Pasadena, California, April 1962, CONFIDENTIAL REPORT

10. W. Hayes and R. Probstein, "Hypersonic Flow Theory," Academic Press, 1959

11. W. R. Hartill and A. E. Heins, "High Compression Hypersonic Inlet Data," Paper presented at AIAA Hypersonic Ramjet Conference, U. S. Navy Ordnance Laboratory, White Oaks, Maryland, April 1963

12. L. Crocco, Fundamentals of Gas Dynamics, Vol. 3 of the "High Speed Aerodynamics and Jet Propulsion", Princeton University Press, 1958

4.0 FUEL INJECTION AND COMBUSTOR ANALYSIS

4.1 INTRODUCTION

To obtain good performance in the Scramjet engine, it is necessary that the fuel mix and react with captured air stream. The contents of this section briefly summarize the conclusions and opinions formed through analytic investigation regarding fuel injection and mixing in Scramjet combustors.

4.2 LIST OF SYMBOLS

E	Eddy Diffusivity
$f'\lambda_c$	Standard Heat Release at the Local Fuel-Air Ratio, f
$\bar{f}'\lambda_c$	Standard Heat Release at the Over-all Fuel-Air Ratio, $\bar{f}$
H	Static Enthalpy, Absolute Basis
j_5	Impulse Function at Combustor Exit
$\dot{m}/A$	Mass Flow Per Unit Area
P	Static Pressure
R_t	Turbulent Reynolds Number
r	Radial Coordinate
U_e	Velocity of External Stream
δ^*	Displacement Thickness
η_c	Over-all Combustion Efficiency
η_m	Mixing Combustion Efficiency
η_R	Reaction Combustion Efficiency
λ_c	Standard Heat of Combustion Per Unit Mass of Fuel

LIST OF SYMBOLS (continued)

μ Fraction Mass Flow

ρ Density

4.3 ON DEFINITIONS OF COMBUSTION AND MIXING PERFORMANCE CRITERION

Many recent detailed investigations of turbulent compressible mixing (Refs. 1, 2, 3)* and combustion reaction analyses (Refs. 4, 5, 6) show evidence of considerable insight, ingenuity, and labor in their solutions. However these results are usually not in a form to be applied directly in most performance cycle analyses, assuming comparable boundary conditions, without considerable labor on the user's part. This is due, in part, to the lack of adequate standards on which to report results and to evaluate them for more general correlations. In this section we shall attempt to describe the essential features of parameters which would best relate theoretical and experimental combustor studies to those used in parametric performance analyses.

All engine cycle computations utilize an efficiency defined as an equivalent heat loss from an equilibrium gas, based on the heating value of the fuel and the fuel-air ratio. Let us consider the case where the composition, temperature, pressure, and density have been computed by a detailed chemical reaction program for a given (uniform) entrance condition to some point where the reaction is not yet in equilibrium. Then the same dynamic situation should be reproduced if the comparable equilibrium gas had the same pressure and density,

*Subject references appear in Section 4.10, page 55.

but with a total enthalpy decreased by a heat loss equal to $(1-\eta_R) f' \lambda_c$. Thus, we can define the combustion reaction efficiency, η_R, for an arbitrary reacting gas at some instant to be

$$\eta_R = 1 - \frac{H(P,\rho,\text{non-eq}) - H(P,\rho,\text{eq})}{f' \lambda_c} \tag{4.1}$$

where the H are computed on an absolute basis. Here f' is the fuel-air ratio for fuel-lean mixtures and is the stoichometric ratio for fuel-rich mixtures while λ_c is the standard heating value per unit mass of fuel.

In the case where there is simultaneously incomplete mixing and incomplete reaction, the balance on the over-all total enthalpy across the duct section and the heat of reaction relation at the reference temperature for λ_c leads to the definition of the over-all heat release efficiency

$$\eta_c = \frac{1}{\bar{f}' \lambda_c} \int_0^1 \eta_R(\mu) f'(\mu) \lambda_c \, d\mu \tag{4.2}$$

where μ is the fraction mass flow. Here $\bar{f}' \lambda_c$ is the reference heat release if the mixture were uniform at the over-all mixture ratio $\bar{f}$. The λ_c inside the integral and in the denominator are the same, hence can be cancelled. Note that if the mixture is everywhere in local chemical equilibrium, then $\eta_R = 1$ and we have the combustion mixing efficiency, η_m given by

$$\eta_m = \frac{1}{\bar{f}'} \int_0^1 f'(\mu) \, d\mu \tag{4.3}$$

This relation states that for the case of instantaneous local equilibrium, the combustion efficiency η_c is equal to the mixing efficiency η_m, and is mixing limited. If the mixture is everywhere less than stoichiometric and the over-all $\bar{f}$ is less than stoichiometric, or alternatively, if the mixture is everywhere greater than stoichiometric and $\bar{f}$ is greater than stoichiometric it follows that

$$\bar{f}' = \int_0^1 f'(\mu)\, d\mu \tag{4.4}$$

and the mixing efficiency η_m is unity. Equation (4.4) implies that the combustion efficiency is now reaction limited. An interesting mathematical theorem derived in Ref. 7 (page 309) may be applied to Eq. (4.2) for the case of hydrogen-air mixing. Generally, it is the capture of air into the turbulent mixing zone which limits the uniformization of the mixture. Hence, we can say roughly that at a given duct length the gases in stream tubes close to the fuel jet centerline have had a longer time to react than those in stream tubes close to the jet boundary. The reaction efficiency should be higher for higher fuel-air ratios f. This would make η_R covariant with f' in the sense that Crocco uses the term and it follows using his theorem that

$$\eta_c > \frac{1}{\bar{f}'}\left(\int_0^1 \eta_R\, d\mu\right)\left(\int_0^1 f'\, d\mu\right) = \eta_m \int_0^1 \eta_R\, d\mu \tag{4.5}$$

In other words, the over-all combustion efficiency η_c is higher than the product of the mean reaction efficiency and the mixing efficiency. Thus, conservative estimates of η_c are obtained by separately computing reaction and mixing efficiency, and multiplying the two efficiencies.

Notice that the reaction and mixing efficiencies are defined in such a manner that they are equivalent to local heat losses in an equilibrium gas. There are other losses associated with incomplete reaction and mixing which occur in the subsequent expansion in the nozzle. These may be classed as nonuniformity effects. These losses, however, are not assigned to the combustor, but are expansion losses properly assigned to the exhaust nozzle, as will be discussed in Section 5.

4.4 ON NONUNIFORMITY AT THE COMBUSTOR EXIT

There are losses in the combustor due to friction and heat transfer to the walls, in addition to the combustion energy losses discussed above. The wall friction is used in the momentum balance along with the pressure-area term (cf., Section 3.6, Eq. (3.8)) to evaluate the combustor exit impulse function j_5. The effective total enthalpy, H_{t_5}, is evaluated from the input total enthalpy less heat loss and over-all combustion efficiency loss defined as in Eq. (4.2). The quantities j_5, H_{t_5}, and $\dot{m}_5/A_5$ are sufficient to characterize the ideal thrust developed in an isentropic expansion. Note that we choose to define quantities which would be constant in an ideal constant area combustor duct. Hence, these quantities are chosen as the reference constants upon which to base the studies of losses. Had we chosen any of the quantities such as mean velocity, kinetic energy, pressure, density, or enthalpy, the evaluation in an ideal constant-area combustor would require the use of the heat, mass, and momentum balance,

implicitly using the quantities j_5, H_{t_5}, and $\dot{m}_5/A_5$ but also requiring further evaluation and definitions of the meaning of mean values. This extra step in analysis leads to some confusion regarding nonuniformity corrections.

Once we have accepted that the basis for comparison is with the same exit conditions in the mean values of impulse function, total enthalpy, and area, then the question as to mean values becomes simply a perturbation analysis. The approach used at NESCO (Ref. 8) is consistent with this viewpoint. Other nonuniformity analyses, especially those using displacement thickness in analogy to boundary layers, can be easily adapted.

4.5 FUEL INJECTION

In a preliminary investigation into simplified theories of jet penetration, experimental data (Ref. 9) on the cross stream penetration of a supersonic jet injected into a supersonic flow were compared with the theories of Lindley (Ref. 9), Ferrari (Ref. 10), and Abramovitch (Ref. 11). The first two theories were for supersonic flow while the last was based on subsonic theory and data. In every case, theory called for penetrations which were far greater by a factor of at least 2 than was actually measured. Physically unrealistic drag coefficients of the order of 50 or more were required to rationalize theory with data. The basic erroneous assumption which lies at the heart of each of the above mentioned theories is that the injectant stream is coherent and quasi-uniform across its diameter. The actual phenomena calls

for an expansion fan on the downstream side of the jet. The theory of Zukoski and Spaid (Ref. 12) does not assume any mechanism for turning. The injected stream immediately turns to flow along the wall. The correlation with their own data is good and comparison with Marquardt data (Ref. 9) is fair. Since the Marquardt work is done under simulated Scramjet conditions, the latter's empirical correlation seems adequate for most purposes.

The data of Zukoski and Spaid on concentration profiles behind a normally injected stream suggest that a vortex filament is shed from both sides. The axis of the vortex is roughly parallel to the wall and has a rotation such that material near the wall is swept toward the center of the injected stream. The slot injector tried by General Electric (Ref. 13), with the long side aligned to the flow, should cause an even stronger pair of vortex filaments to be formed. The slot injector obtained better mixing than the circular injector for the same pressure and flow rate. These vortex filaments increase the amount of initial mixing, but the influence also seems to die down rather rapidly since the data reported in Ref. 5 with flush wall injection at Mach 2.3 show little improvement in mixing with distance downstream. These preliminary experiments suggest that shaped slot injectors can be designed which would create a stronger single whirl, rather than a pair, hence leading to more persistent and effective vortex mixing.

At small angles of inclinations of the injected stream to the main stream, the vortex filaments do not appear to form and penetration is better (Ref. 13). It is conjectured that strong vortex

formation will be associated with the oblique shock formed near the base of the injected jet. If this shock wave is a strong oblique wave, rather than a weak attached oblique shock then there seems a greater tendency to form vortices. Hence, the amount of initial mixing induced by the act of injection should be quite different when correlated with the effective deflection angle of the forward face of the jet.

The expansion of the injected fuel stream, where the fuel injector pressure is much higher than the combustor entrance air static pressure, will cause oblique shock waves to form. If the blockage is sufficiently large then separation in the boundary layer ahead of the injection point will occur. Such separation by itself does not affect the over-all combustor momentum balance and over-all performance unless it affects pressure on convergent or divergent walls.

Downstream of the injection point, certain local restrictions on allowable fuel injection conditions may occur. They are that the over-all mass, momentum, and energy balance, either before or after heat release, do not reach choking conditions. Certain other limiting conditions previously reported in Refs. 8 and 14 were based on the assumption of uniform pressure across the combustor. These limiting conditions were found to be easily relieved if the pressures are allowed to be unequal in the unmixed or partially mixed fuel and air stream, hence are not true limits on injector configurations.

4.6 MIXING STUDIES

The problem of mixing of supersonic jets have been investigated

in a series of studies (Refs. 8, 14, 15, 16). The starting point for all of these analyses were the boundary layer assumptions. As reported in Ref. 16 the basic assumption of the cross stream pressure gradients being negligible is suspect, but there is no simple method for including this in mixing analyses. The assumption that cross stream pressure variations have a secondary effect on the local spreading angle, relative to the local velocity vector seems a reasonable one (Ref. 8). It is conjectured that analyses that do include the pressure effects will show increases in the over-all mixing rate, but the effect would be hard to separate from injection effects.

The investigations have been centered mainly around the use of the integral method of solving free mixing problems. In addition to the usual equations for the conservation of mass, momentum, fuel mass, and energy, the integral equation formed from the moment of fuel mass conservation was used to determine the rate of spread (Ref. 14). It is necessary to assume profile distribution functions for velocity, total enthalpy and fuel mass fraction, and that this profile function is similar throughout the length of the jet. Based on supersonic wall boundary layer experience, it was assumed that the proper basis for similarity is the Howarth radial coordinate, and on the basis of Abramovitch's experience in subsonic mixing that Schlichting's wake profile function was applicable (Ref. 14). Comparison with data from the Marquardt Corporation (Ref. 5) and the General Electric Company (Ref. 13) showed that the first assumption, while requiring some further checks, is substantially correct, but that the second assumption,

coupled with the first, is wrong. The profile function for hydrogen mixing with air in the absence of reaction is considerably closer to being Gaussian than the polynomial expression of Schlichting. Fortunately, it turns out that rather crude forms of the profile function lead to fairly good approximations to the spreading rate. This is, in fact, one of the primary advantages of the integral formulation.

Solutions based on the vonMises transformation (Ref. 1, 2) were not used since the solutions corresponding to small external velocity are not correct, hence could not be compared to most of the subsonic data on jet spreading.

Various forms of the eddy diffusivity formulation were investigated. The basic form which seems adaptable to both low-speed wall boundary layers and to mixing of fluids of different density is that based on a displacement thickness. It is provisionally defined as

$$\overline{\rho E}(x) = \frac{\rho_e u_e \delta^*}{R_t} = \frac{1}{R_t}\int_0^s (\rho_e u_e - \rho u)\, dr \qquad (4.6)$$

Here R_t is a constant which in two-dimensional subsonic jets takes on the value 62. The form is not inconsistent with that proposed by Ferri (Ref. 17), but is in the form of an integral rather than an over-all mean difference. It has been shown (Ref. 14) that the Eq. (4.6) reduces to Ferri's form for low speed nonreactive flow, and to Prandtl's classic relation for the exchange coefficient for constant density flow.

Most mixing studies have assumed that longitudinal pressure gradients are negligible. However, in constant-area supersonic combustion ducts, the pressure rise can be quite large, especially at

lower flight speeds. A theoretical study to include these effects of pressure gradient in a variable area duct are reported in Ref. 18.

A comparison between theory and data obtained by the Marquardt Corporation (Ref. 9) in cold flow tests on the mixing of hydrogen with nitrogen are shown in Figure 4.1. Mole fraction of hydrogen at the centerline is plotted as a function of the distance downstream. Examination of the figure shows that the predicted centerline distribution is somewhat flatter than the experimentally observed distribution. Better correlation could be obtained by using a slightly smaller value of the turbulent Reynolds number, R_t. Considering that the Reynolds number was evaluated for subsonic jets of air in a quiescent atmosphere, the comparison is regarded as being reasonably good.

It was found that mixing is more rapid in constant area ducts than in constant pressure ducts, as shown in Figure 4.2. Here, half-width of mole fraction, mass fraction, and total width are compared for two different assumptions regarding the pressure-area distribution. Due to the density term appearing in the eddy viscosity formula (Eq. (4.6)) the increase in pressure with mixing increased the eddy diffusivity, hence decreased the mixing distance. In another case the effect of shock-waves was simulated by using a total pressure drop in the outer stream. It will be noted that the distance required for the mixing zone to reach the wall is increased with total pressure loss in the outer stream, as shown in Figure 4.3. This would indicate a combustor length trade-off between oblique shock waves caused by the fuel injector, and the shear-controlled mixing rate. However, the increased mixing due to the injector,

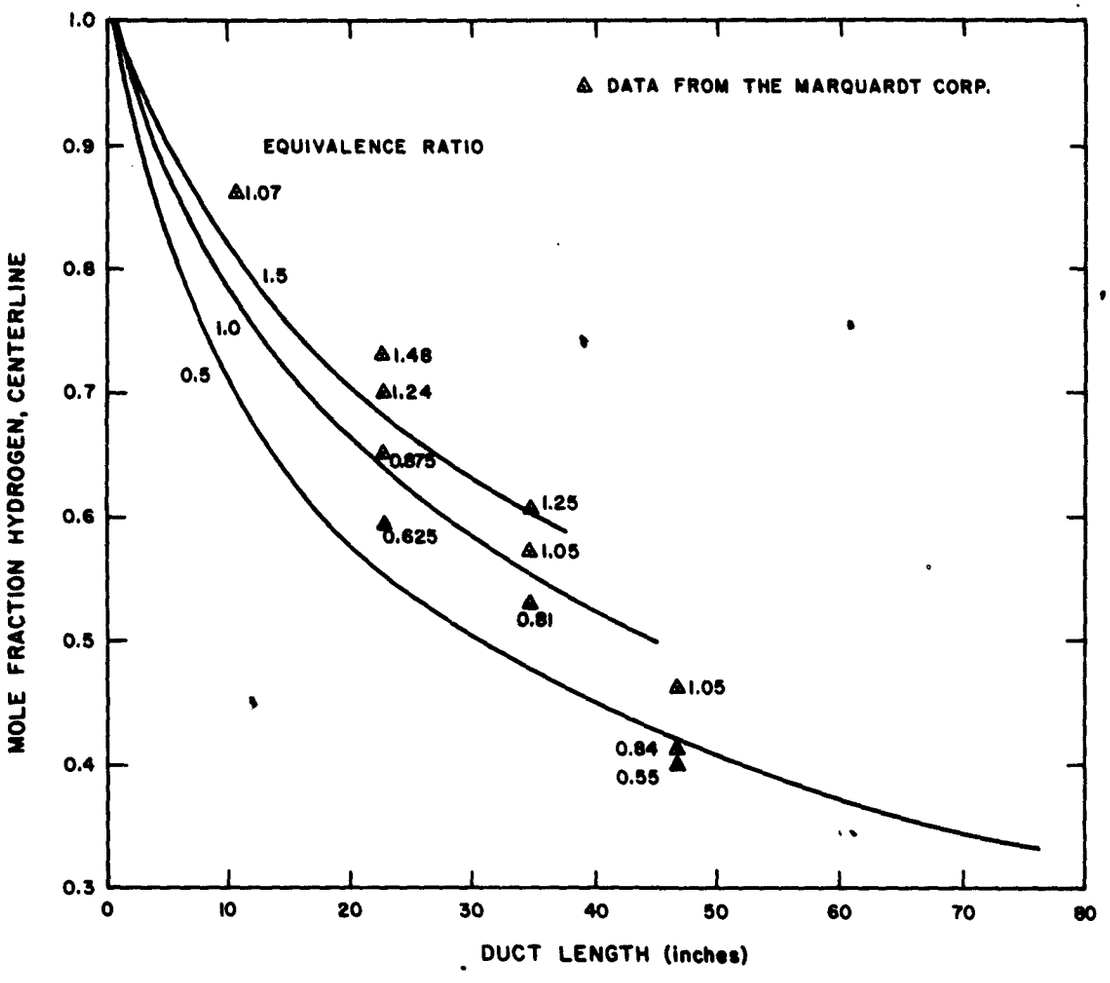

FIGURE 4.1

CENTERLINE FUEL DISTRIBUTION

$M_{air} = 2.3$ $M_{fuel} = 2.0$ $h_{t_f} / h_{t_a} = 14.0$ $A_f / A_a = 0.0173$

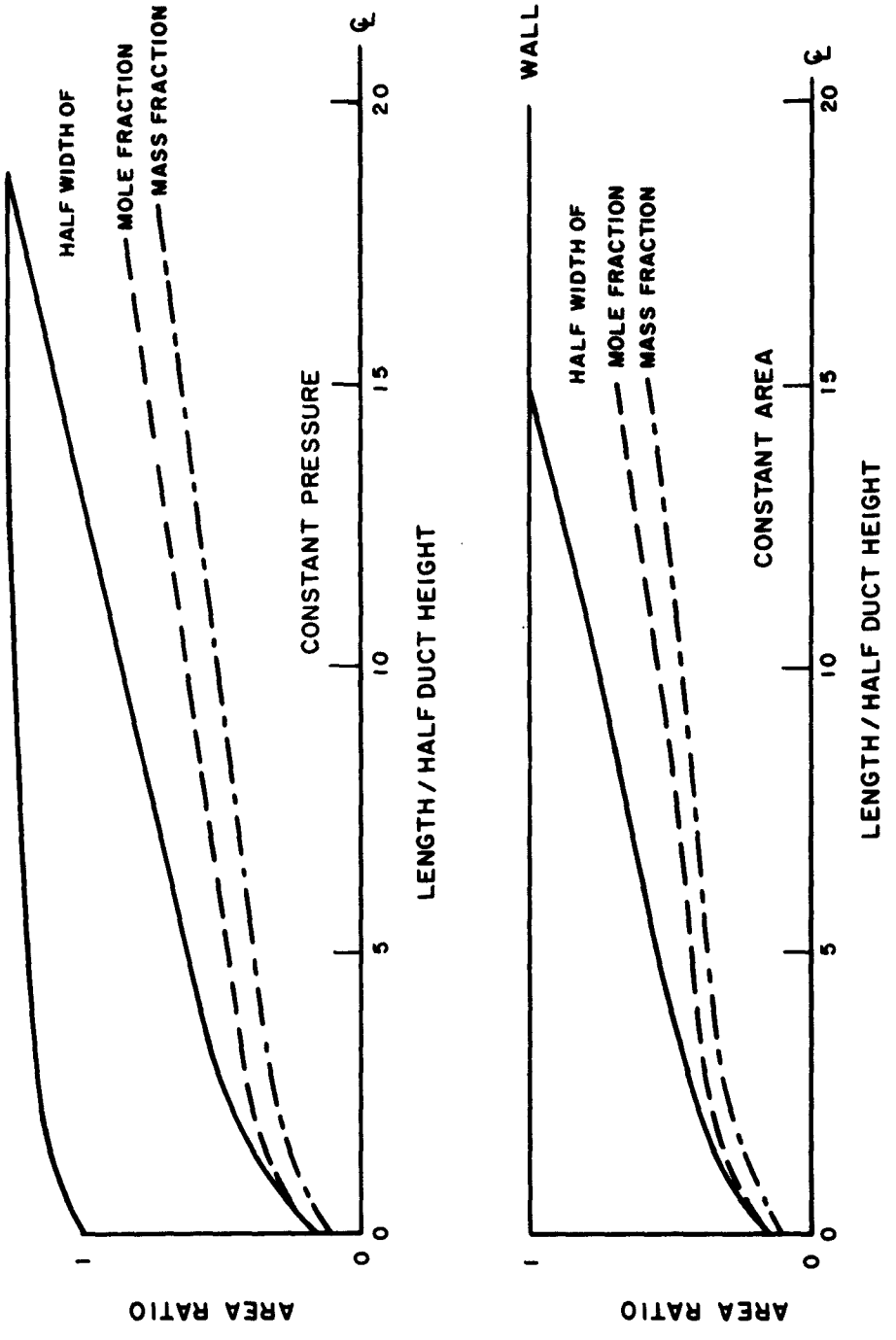

FIGURE 4.2
CHARACTERISTIC WIDTHS OF CONFINED JETS $M_{air} = 2.3$, $M_f = 1.0$
$h_{t_f}/h_{t_a} = 14.0$, $A_f/A_a = 0.0173$, E. R. = 1.0

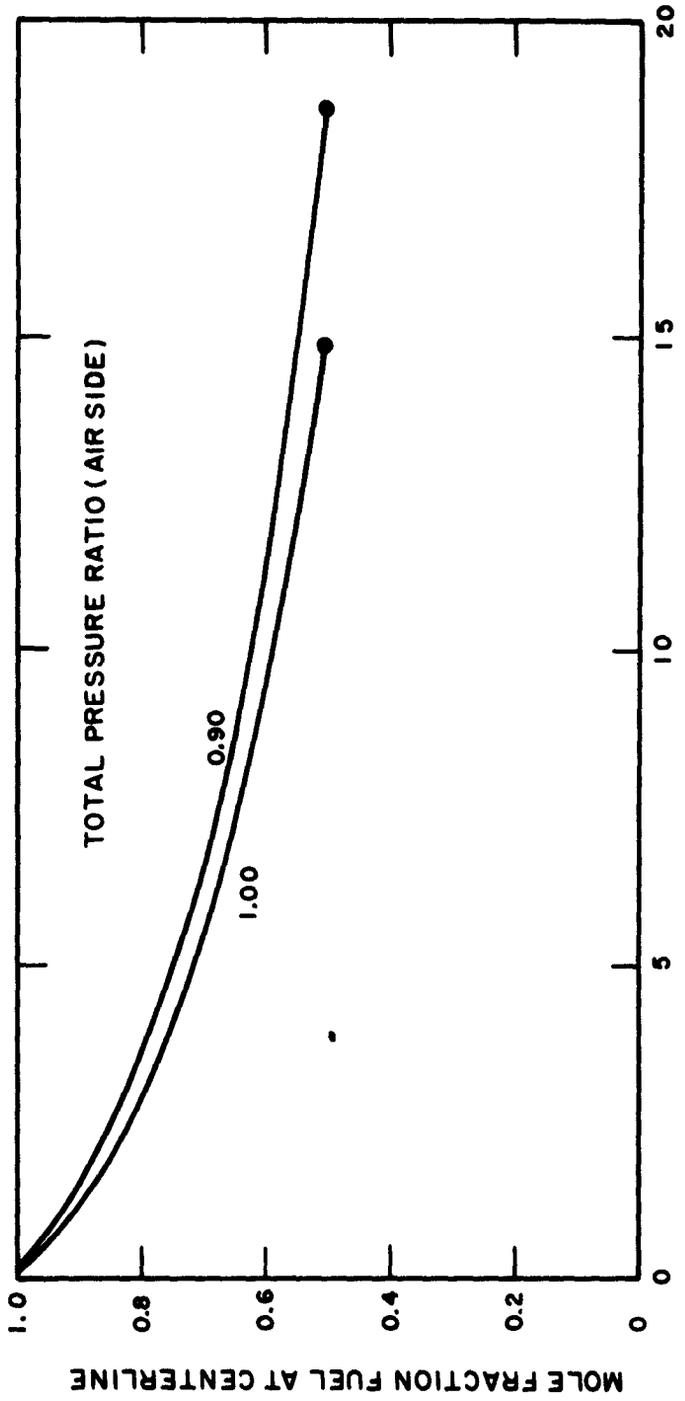

FIGURE 4.3
EFFECT OF TOTAL PRESSURE LOSS ON LENGTH FOR MIXING TO REACH WALL
$M_{air} = 2.3$, $M_{fuel} = 1.0$, $h_{t_f} / h_{t_a} = 14.0$, $A_f/A_a = 0.0173$

which is not considered here, and offset this loss.

The integral theory of free mixing analysis, while convenient and rapid, is not easily adapted to the study of simultaneous mixing with finite rates of chemical reaction. The integral analysis requires that the profile functions of the reacting species be known. While a general polynomial function can be assumed with coefficients to be evaluated as part of the solution, reliable results would require a high order polynomial. The direct numerical solution of the controlling partial differential equations, while time consuming, would probably be easier to program for computers. The validity of such solutions, however, depend very strongly on the validity of the eddy diffusivity relation. It would be of interest to investigate some simple configurations for comparison with experiments.

4.7 CONSTANT PRESSURE MIXING STUDIES

Fundamental studies on the possible transformations of the equations of compressible turbulent mixing with reaction to that of an analogous incompressible mixing problem were reported in Ref. 14. In brief, it has been shown that transformation of the partial differential equations of motion are not possible except with physically implausible assumptions regarding the shear stress term. However, it is possible to obtain a transformation of the integral form of the equations of motion. As a consequence it is theoretically possible to correlate low-speed diffusion flame data with supersonic data. Proof of the validity of the transformation is obtained in the prediction of core

length in axisymmetric jets, as was shown in Ref. 14.

The transformation theory was applied to the problem of a two-dimensional constant pressure diffusion flame with equilibrium gas properties. These results were reported previously in Ref. 14. An example was computed with air at a velocity of 3500 fps, hydrogen fuel injected at 3000 fps, air and hydrogen static temperature of 1650°R, and 1000°R respectively, and a static pressure of 2 atmospheres. Exact equilibrium gas properties were used for this computation. Profiles of velocity, composition, temperature, and Mach number were obtained. Due to the length of time required to compute one case (70 minutes machine time), no further examples were computed.

4.8 CONCLUSIONS

1. Neither theoretical nor experimental data on reaction and mixing were found to be reporting data in a manner consistent with usage in cycle analyses. A definition of combustion efficiency as equivalent heat loss in an equilibrium gas at the same pressure and density is proposed.

2. Fuel jet penetration into supersonic streams cannot be correlated with theories which depend on the drag to turn the injected stream. Theories which do not depend on drag, but on Prandtl-Meyer expansion of the injected stream seems more successful.

3. Integral methods of analyses for mixing in variable area ducts have been developed. Constant area ducts exhibit more rapid mixing than divergent, constant pressure ducts. Fairly good correlation with experimental data have been obtained.

4.9 RECOMMENDATIONS

1. Further work on correlating integral mixing analyses with experimental data in constant area ducts is required.

2. A more general analyses to include effects of wall boundary layer and multiple injection is possible and should be undertaken.

4.10 REFERENCES

1. Libby, P., "Theoretical Analysis of Turbulent Mixing of Reactive Gases with Application to Supersonic Combustion of Hydrogen," ARS Jour. Vol. 32, No. 3 (1962).

2. Schetz, J., "Supersonic Diffusion Flames," 21st AGARD Combustion and Propulsion Panel, London (1963).

3. Vasiliu, J., "Turbulent Mixing of a Rocket Exhaust Jet with a Supersonic Stream Including Chemical Reaction," Jour. Aerospace Sciences, Vol. 29, No. 1 (1962).

4. Momtchiloff, I.N., Taback, E.D., Buswell, R.F., "Kinetics of Hydrogen-Air Flow Systems," Ninth Symposium on Combustion, pp. 220-230, Academic Press (1963).

5. "Applied Research and Advanced Technology of the Supersonic Combustion Ramjet Engines (U)," Tech. Doc. Rept. No. APL-TDR-64-44, The Marquardt Corp., Van Nuys, California, July 1963. SECRET REPORT.

6. Pergament, H. S., "A Theoretical Analysis of Nonequilibrium Hydrogen-Air Reaction in Flow Systems (U)," General Applied Science Laboratories, Westbury, L.I., New York, Tech. Rept. No. 325, Nov. 1962. CONFIDENTIAL REPORT.

7. Crocco, L., Fundamentals of Gas Dynamics, Vol. 3 of the "High Speed Aerodynamics and Jet Propulsion," Princeton University Press (1958).

8. "Advanced Air-Breathing Engine Study (U)," First Quarterly Report, National Engineering Science Co., Pasadena, Calif., 6 March to 6 June 1963, Contract No. AF 33(657)-10794. CONFIDENTIAL REPORT.

9. "Annual Report - Aerospace Propulsion Program, Vol. VI, Supersonic Combustion Ramjet (U)," Marquardt Corp., Van Nuys, Calif., Report No. 5883, March 1962. CONFIDENTIAL REPORT.

10. Ferrari, C., "Interferences Between a Jet Issuing Laterally From a Body and the Enveloping Supersonic Stream," Johns Hopkins University, Applied Physics Lab., Bumblebee Report No. 286, April 1959. Unclassified

11. Abramovitch, G. H., "Turbulent Jet Theory," Rough Draft Translation from Russian, A. D. 283858.

12. Zukoski, E. E. and Spaid, F. W., "Secondary Injection of Gases into a Supersonic Flow," Presented at AIAA Solid Rocket Propellant Meeting, Jan. 29-31, 1964.

13. "Advanced Air-Breathing Engines (U)," Vol. I-II, APL-TDR-64-21, General Electric Co., Evendale, Ohio, 7 May 1964. SECRET REPORT.

14. "Advanced Air-Breathing Engine Study (U)," Second Quarterly Report, National Engineering Science Co., Pasadena, Calif., Tech. Doc. Rept. No. APL-TDR-64-16, Contract No. AF 33(657)-10794, April 1964. CONFIDENTIAL REPORT.

15. Kubota, T., "Integral Method for Supersonic Diffusion Flames," National Engineering Science Co., Pasadena, California, Tech. Note No. 2, (1962).

16. "Advanced Air-Breathing Engine Study (U)," Final Report, National Engineering Science Co., Pasadena, California, Tech. Doc. Rept. No. ASD-TDR-62-1093, Contract No. AF 33(657)-9244, April 1963. CONFIDENTIAL REPORT.

17. Ferri, A., Libby, P.A. and Zakkay, V., "Theoretical and Experimental Investigation of Supersonic Combustion," Polytechnic Institute of Brooklyn, PIBAL Report No. 713, September 1962.

18. Kushida, R., "Supersonic Mixing in Variable Area Ducts (U)," Technical Report No. 129-4, National Engineering Science Company, Pasadena, California, July 1964. CONFIDENTIAL REPORT.

5.0 EXHAUST NOZZLE STUDIES

5.1 INTRODUCTION

The nozzle for a supersonic combustion ramjet presents analytical problems that are somewhat different from those encountered in conventional rocket nozzles. Due to the supersonic velocity at the nozzle entrance, the thrust increment obtained from such a nozzle is smaller than the comparable conventional nozzle with sonic throat velocity. Velocity and enthalpy nonuniformities across the combustor exit, due to incomplete mixing of fuel and air, are no longer suppressed by thermal choking. In addition to the problems arising from the supersonic velocity, high combustion temperatures are responsible for dissociation of the chemical species in the gases entering the nozzle. The resulting chemical recombination and heat release in the nozzle makes the gasdynamical analysis of the flow more uncertain. The nozzle design will probably be asymmetric because of unorthodox inlet designs and over-all engine envelope requirements.

The theoretical studies conducted at NESCO on nozzle performance are presented in this section and can be summarized as,

a) examination of nozzle contours of limited length designed for optimum thrust

b) evaluation of loss in thrust due to nozzle wall friction

c) location of "sudden-freezing" line in the nozzle and its influence on nozzle thrust performance

d) changes in nozzle thrust performance due to nonuniformities at nozzle entrance

e) evaluation of lift force on the nozzle due to asymmetric contour or nonuniform entrance flow conditions.

The theoretical approach used in nozzle flow analysis and discussion of the computational results are given in the following subsections.

5.2 LIST OF SYMBOLS

A	Nozzle Cross-sectional Area
dA	Elemental Area of Control Surface
C_{Ej}	Exit Impulse Efficiency
C_{Nj}	Nozzle Impulse Coefficient
h	Enthalpy
j	Stream Thrust Per Unit Mass Flow
$\dot{m}$	Mass Flow Rate Through Nozzle
$d\dot{m}$	Elemental Mass Flow Through Elemental Area of Control Surface
P	Pressure
s	Coordinate Along Stream Line
V	Velocity
X	Axial Coordinate
Y	Nozzle Cross-section Height Also Equal to Cross-section Area A in the Case of Two-dimensional Nozzles
θ	Isentropic Exponent
γ	Velocity Direction

Subscripts

a, b, c Average Flow Conditions Across Each of the Stream Tubes a, b, and c (see Figure 5.8)

i Reference Value Reached by One-dimensional Flow

5 At Nozzle Entrance (also equal to subscript "throat")

6 At Nozzle Exit

5.3 NOZZLE PERFORMANCE PARAMETERS

The primary purpose of a nozzle, which is to impart momentum to the exhaust gases as they leave the nozzle exit, can be evaluated by considering the exit impulse. Let us denote by subscript 6 the flow conditions along a control surface at the nozzle exit and normal to the thrust axis as indicated in Figure 5.1. Because, in general, the nozzle length is limited, the flow conditions at the exit control surface would be nonuniform and one can write

$$\text{Nozzle exit stream thrust} = \int_0^{A_6} P\,dA + \int_0^{\dot{m}} V \cos\theta\, d\dot{m} \qquad (5.1)$$

where P = static pressure
$d\dot{m}$ = elemental mass flow
V = velocity
θ = flow direction

across an elemental area of dA of the control surface. The integration is taken along the control surface across the nozzle exit area A_6 and encompasses the entire mass flow $\dot{m}$ through the nozzle. The above Eq. (5.1) gives us the component of exit stream thrust in the thrust

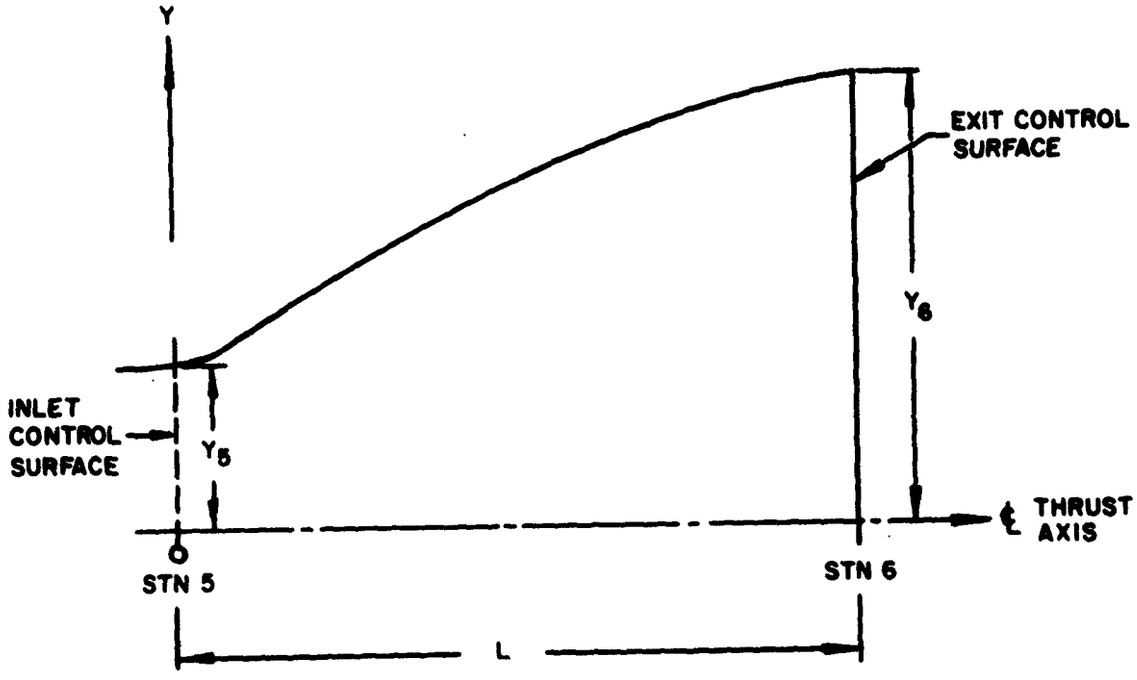

FIGURE 5.1
SCHEMATIC OF EXIT NOZZLE CONFIGURATION

axis direction.

Similarly, one can write

$$\text{Nozzle entrance stream thrust} = \int_0^{A_5} P\,dA + \int_0^{\dot{m}} V \cos\theta\, d\dot{m} \qquad (5.2)$$

where the integration is taken along a control surface at the nozzle entrance area A_5

Mass flow of exhaust gases crossing the control surface at nozzle entrance should be equal to mass flow across the control surface at nozzle exit. Hence

$$\dot{m} = \int_0^{A_5} d\dot{m} = \int_0^{A_6} d\dot{m} \qquad (5.3)$$

It is found convenient to use stream thrust per unit mass flow as a parameter denoted j. Hence

$$j_6 = \frac{1}{\dot{m}} \left[\int_0^{A_6} P\,dA + \int_0^{\dot{m}} V \cos\theta\, d\dot{m} \right] \qquad (5.4)$$

$$j_5 = \frac{1}{\dot{m}} \left[\int_0^{A_5} P\,dA + \int_0^{\dot{m}} V \cos\theta\, d\dot{m} \right] \qquad (5.5)$$

The influence of the divergent portion of the exit nozzle is to increase the stream thrust parameter from j_5 at nozzle entrance to j_6 at nozzle exit.

For prescribed nozzle entrance conditions the value of j_6 depends upon the properties of exhaust gases and nozzle geometry such as expansion ratio, length, and wall contour. The latter effect, i.e., the

influence of nozzle geometry, can be examined by considering nozzle impulse coefficient expressed as

$$C_{N_j} = \frac{j_6}{j_5} - 1 \tag{5.6}$$

In considering the above coefficient one should remember that j_5 is held constant. The exit impulse function j_6 can be computed by analysis of supersonic flow in the nozzle utilizing an appropriate constant value of γ to represent expansion process of the exhaust gases. The effect of nozzle wall friction also can be included in the evaluation of j_6. On the other hand, the influence of flow nonuniformities, frictional and non-equilibrium losses can be brought into focus by examining the exit impulse efficiency defined as

$$C_{E_j} = \frac{j_6}{j_{6i}} \tag{5.7}$$

In the above equation, j_{6_i} is the one-dimensional value for equilibrium expansion of exhaust gases from uniform conditions at nozzle entrance to the particular value of A_6/A_5 under consideration.

The above defined exit impulse efficiency is suitable to study the performance of a given nozzle, whereas the nozzle impulse coefficient as defined by Eq. (5.6) takes into account, also, changes in nozzle area ratio.

However, as can be seen in the following subsections, the nozzle impulse coefficient charts can be easily prepared from nozzle flow

analyses carried out at an appropriate constant value of γ. The more complicated computations, including nonuniform entrance conditions and nonequilibrium losses, can be evaluated only in terms of a prescribed nozzle geometry.

5.4 PARAMETRIC STUDY OF NOZZLE IMPULSE COEFFICIENT

Depending upon the SCRJ engine and vehicle configuration, the exit nozzle could be simple conical, axially symmetric, asymmetric two-dimensional, or three-dimensionally asymmetric. To obtain representative values for performance and its dependency on nozzle area ratio and length,two-dimensional asymmetric nozzle contours are examined. The lower wall of the two-dimensional nozzle is considered plane and parallel to the thrust axis, i.e., combustion chamber centerline. The upper wall of the nozzle between the nozzle entrance and exit is contoured so as to yield optimum thrust. In the case of two-dimensional nozzles, Rao's method (Ref. 1)* for contouring the wall for optimum thrust becomes simple in that they form truncated portions of contours designed for appropriate uniform exit Mach numbers. In the case of axisymmetric nozzles such is not the case and wall contour computations have to be carried out for each individual area ratio and length. It is for this reason that the performance evaluation given here is based on two-dimensional asymmetric nozzles.

Nozzle thrust performance has been computed for several families of two-dimensional optimal nozzles for two nozzle entrance conditions encountered on a typical flight trajectory. The trajectory

*Subject references appear in Section 5.12, page 109.

points and associated nozzle entrance conditions were furnished by the Marquardt Corporation. Appropriate data are listed below for the two points. The first is a moderately low point along the trajectory and the second is near the upper end.

Freestream Conditions		
Speed (ft/sec)	15,000	26,000
Altitude (ft)	130,000	166,000
Nozzle Entrance Conditions		
Mach number	3.31	4.02
Pressure (atm)	1.064	0.444
Temperature (°R)	5,640	7,360
Isentropic exponent	1.105	1.179

Optimal inviscid nozzle contours were machine computed by the method of characteristics using Rao's optimizing technique.

The nozzle flow field computations were carried out utilizing the method of characteristics. The details of the procedures employed are given in Ref. 2. Application of this method to nonequilibrium flow of exhaust gases is much too complicated to be of use in parametric evaluation of nozzle configurations. Hence the exhaust gases are assumed to behave as ideal gas with the appropriate values of γ listed above. For similar reasons, the flow conditions at the nozzle entrance section are considered uniform for the parametric study. However, the influences of nonuniformities at entrance, and nonequilibrium expansion process are evaluated for a typical nozzle configuration in a later subsection.

Nozzle contours for inviscid isentropic flow were computed using Rao's thrust optimization technique and computing machine programs. The details of the procedures are given in Ref. 3. These nozzle configurations are shown in Figures 5.2 and 5.3 for the two nozzle entrance conditions. Superimposed on these figures are lines of constant nozzle impulse coefficient C_{Nj}. The representation used in these figures allows us to choose the nozzle configuration that yields optimum thrust within a prescribed length.

The results presented in Figures 5.2 and 5.3 pertain to only inviscid flow. The influence of viscosity is assumed to affect the flow in a narrow region called boundary layer, near the nozzle wall. Following the well known concepts of boundary layer theory one can compute the mass flow defect and the momentum defect of the flow confined in the boundary layer along the wall. The boundary layer is assumed compressible and turbulent. The boundary layer at the nozzle entrance section is assumed equal in thickness to the boundary layer seven feet behind the leading edge of a flat plate. Nozzle wall temperature was taken into account in the boundary layer equations by the inclusion of a parameter

$$\xi_w = \frac{h_w}{h_t} - 1$$

At each of the two flight conditions ξ_w is assigned a value such that the nozzle wall temperature would be 2680°R. The growth of the boundary layer along the nozzle wall is computed taking into account the local flow conditions obtained from the inviscid flow computations. The details

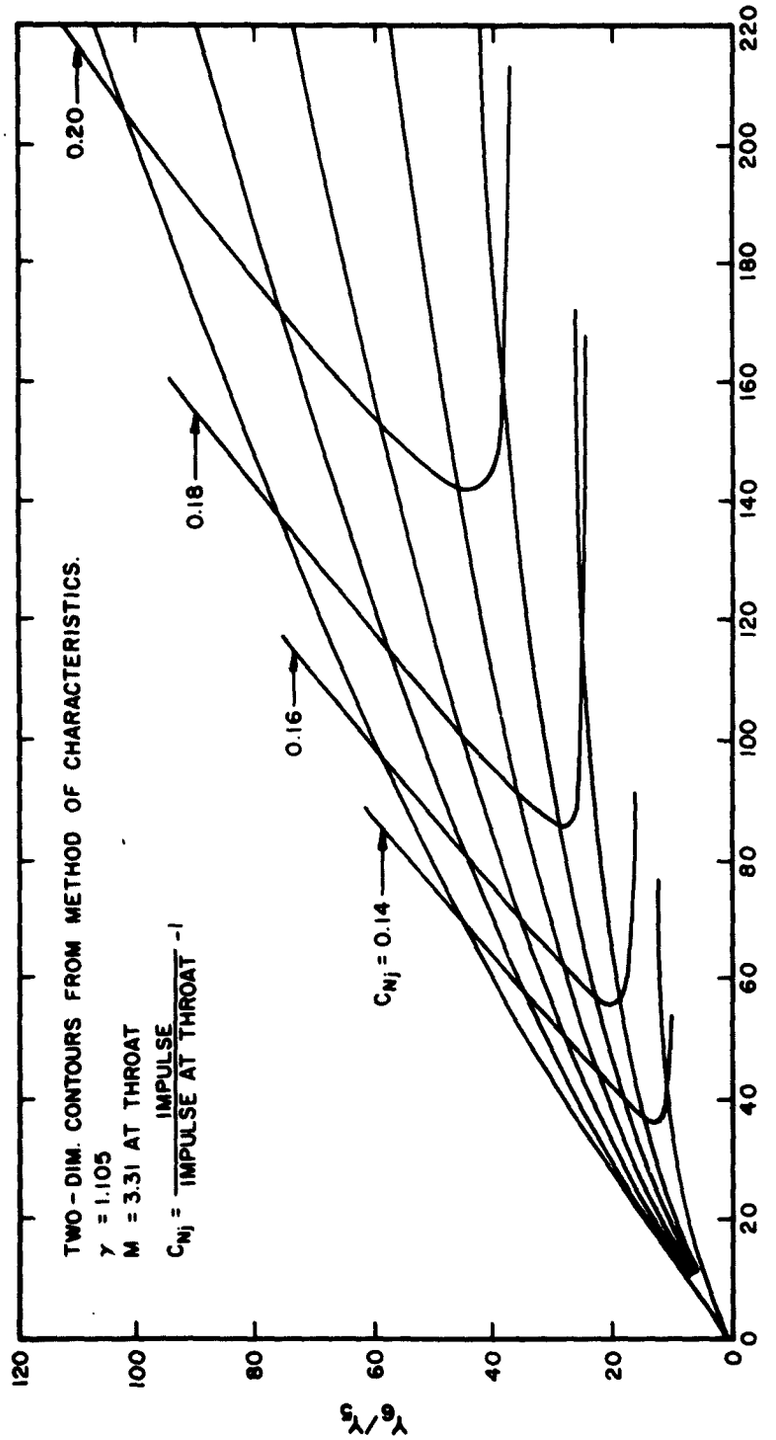

FIGURE 5.2
NOZZLE IMPULSE COEFFICIENT CHART FOR INVISCID FLOW
M_5 = 3.31, γ = 1.105

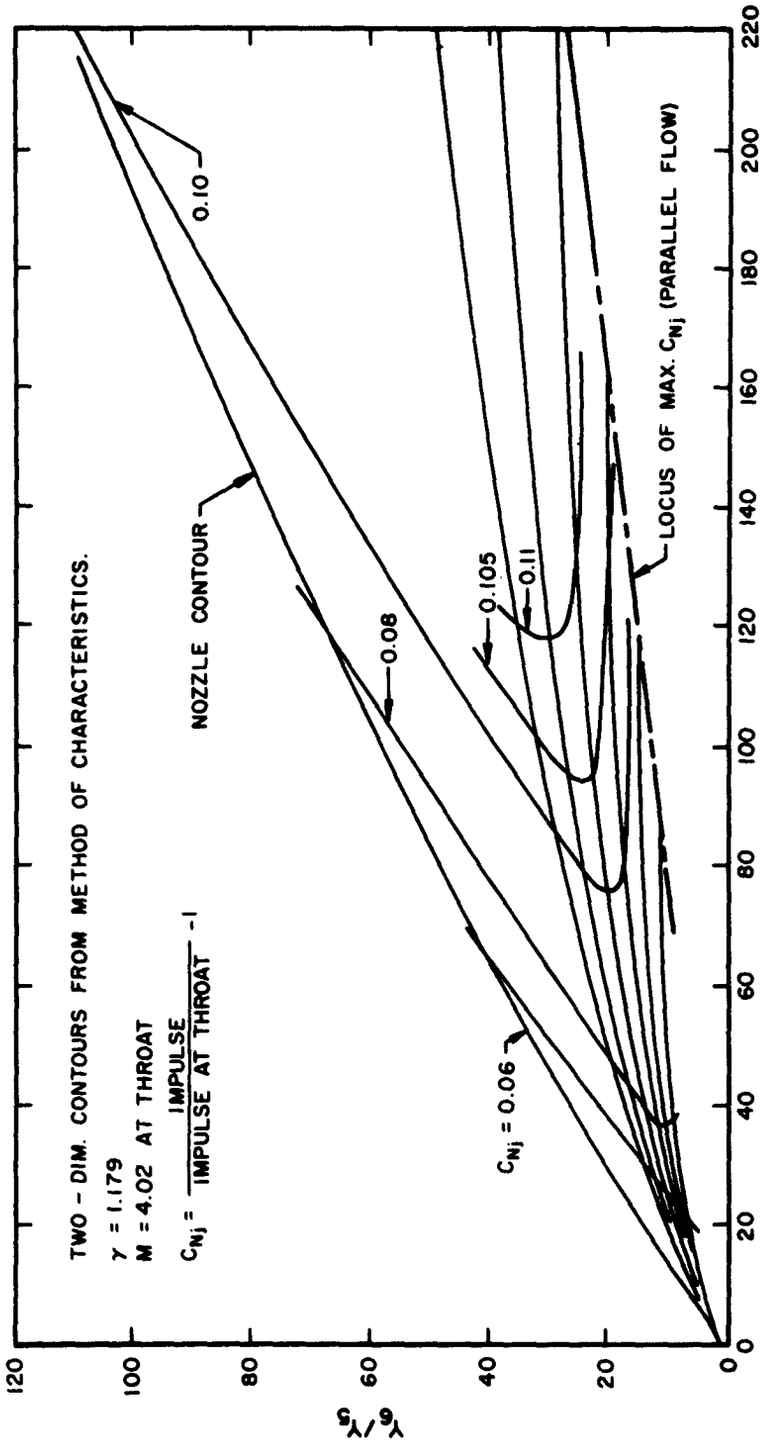

FIGURE 5.3
NOZZLE IMPULSE COEFFICIENT CHART FOR INVISCID FLOW
M_5 = 4.02, γ = 1.179

of analysis and computational procedures for the boundary layer are given in Ref. 4. Only the pertinent results are briefly discussed here. From the boundary layer computations the displacement thickness is computed along each nozzle wall contour shown in Figures 5.2 and 5.3 for the respective flow conditions along the wall. Following the procedure employed in wind tunnel nozzle designs, one can enlarge the cross-sectional areas of the inviscid nozzle contour by the amount of displacement thickness, as shown in Figure 5.4, and expect to have the inviscid flow field left unaltered. The nozzle contours thus corrected for the boundary layer displacement thickness are shown in Figures 5.5 and 5.6.

From the inherent assumption of constant static pressure normal to the wall within the boundary layer, the wall pressures for the contours shown in Figures 5.5 and 5.6 can be obtained from wall pressures computed for inviscid flow in nozzle configurations shown in Figures 5.2 and 5.3. Thus, one can evaluate

$$\int_{A_5}^{A_6} P\,dA$$

the integral of pressure forces on the divergent portion of the nozzle wall is carried out from A_5 up to the exit area A_6*, which now includes the boundary layer displacement thickness at the nozzle exit. The frictional forces on the nozzle wall contribute to a decrement in thrust. By an

*In the case of two-dimensional nozzles, cross-sectional area A and cross-section height y are interchangeable in the following discussion.

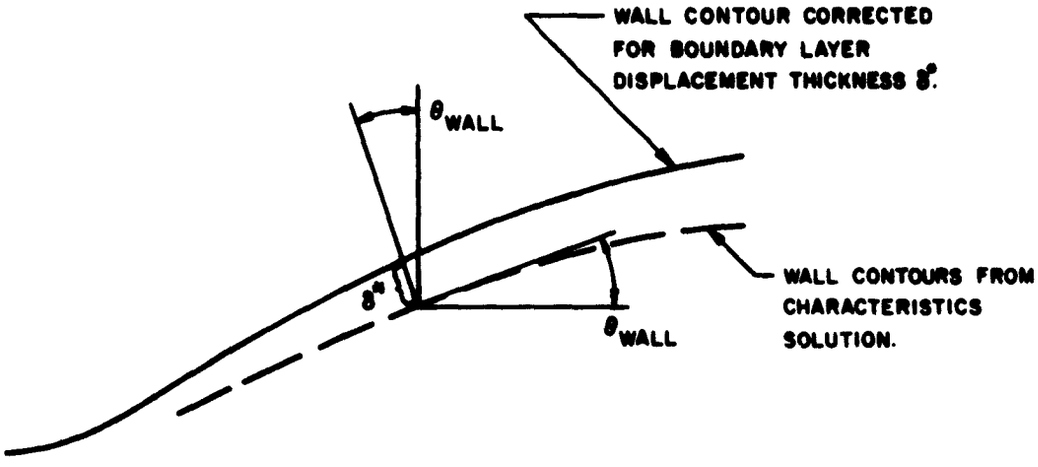

FIGURE 5.4
SKETCH SHOWING THE ACCOMMODATION FOR BOUNDARY DISPLACEMENT THICKNESS

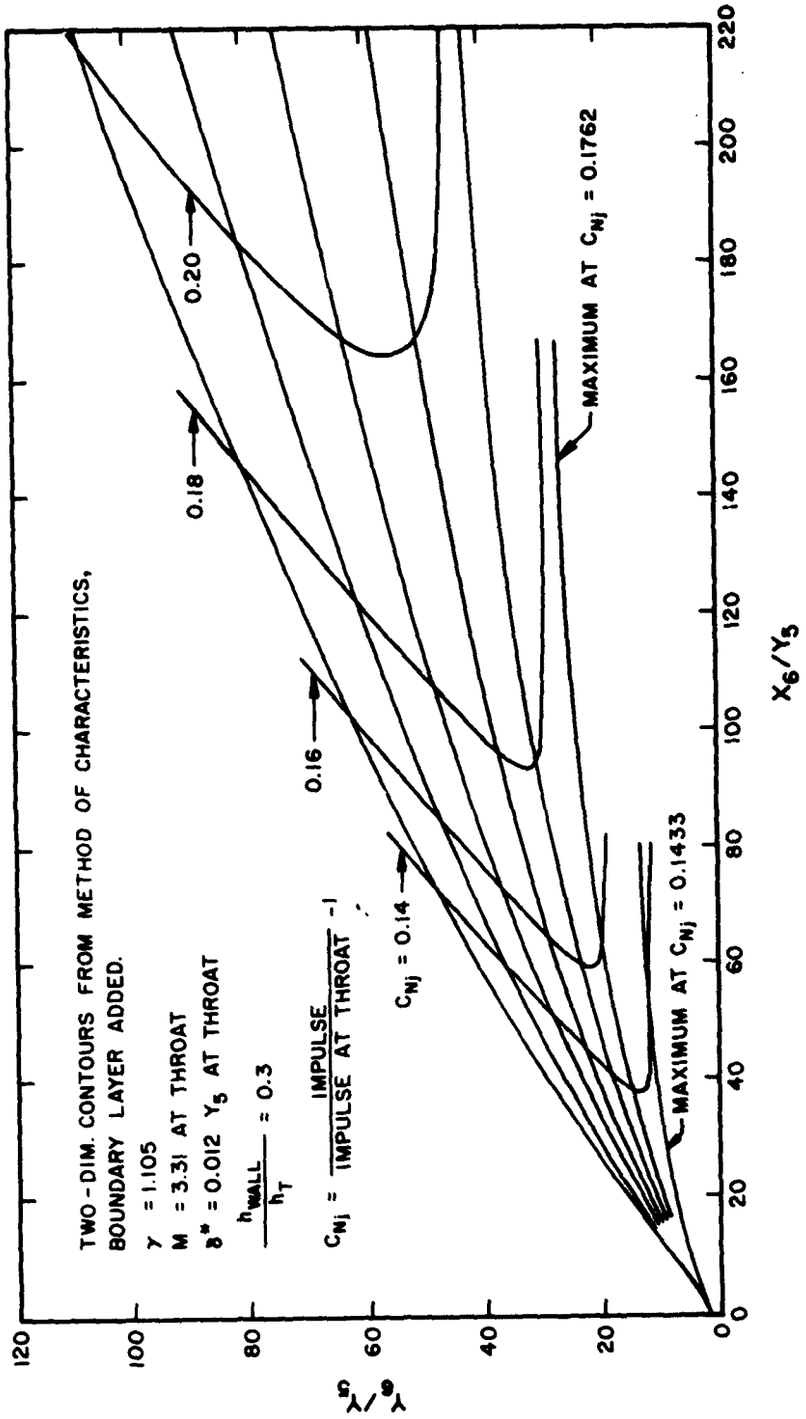

FIGURE 5.5
NOZZLE IMPULSE COEFFICIENT CHART INCLUDING THE EFFECT OF FRICTION
$M_5 = 3.31$, $\gamma = 1.105$

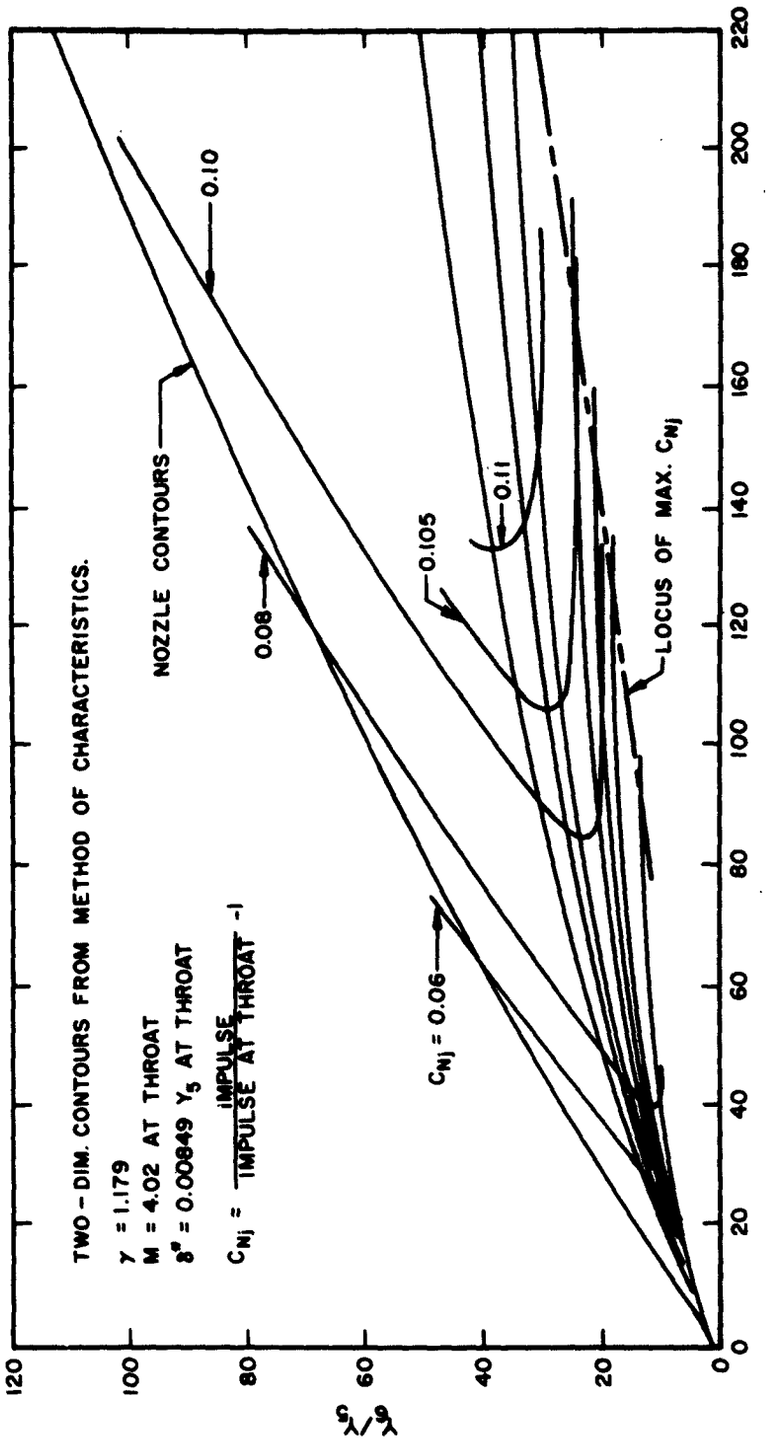

FIGURE 5.6
NOZZLE IMPULSE COEFFICIENT CHART INCLUDING THE EFFECTS OF FRICTION
$M_5 = 4.02$, $\gamma = 1.179$

appropriate choice of friction coefficient applicable to the exhaust nozzle of the SCRJ engine, the frictional losses can be evaluated. A detailed discussion of the choice of the friction coefficient is given in Ref. 3. The exit impulse of the nozzle contours shown in Figures 5.5 and 5.6 can now be computed as

$$j_6 = j_5 + \int_{A_5}^{A_6} P\,dA \text{ - wall friction drag} \qquad (5.8)$$

The nozzle impulse coefficient

$$C_{Nj} = \frac{j_6}{j_5} - 1$$

can represent the influence of nozzle configuration and viscous losses when j_6 is computed according to the above definition. The values of C_{Nj} thus computed for the respective contours at the two flight conditions are also shown in Figures 5.5 and 5.6 by drawing constant C_{Nj} lines.

When we examine nozzle contours of various lengths, but of same exit area we find that beyond a certain length the decrement in nozzle impulse coefficient due to wall friction overcomes the gain due to lower flow divergence losses. Thus, for a given area ratio there is an optimum value of C_{Nj} attainable. These values are indicated in Figures 5.5 and 5.6 for the two families of nozzle contours computed for the two flight conditions. In Figure 5.7, a comparison of C_{Nj} values for one-dimensional, and contoured nozzles is shown. The influence of wall friction losses on C_{Nj} is also shown in the figure.

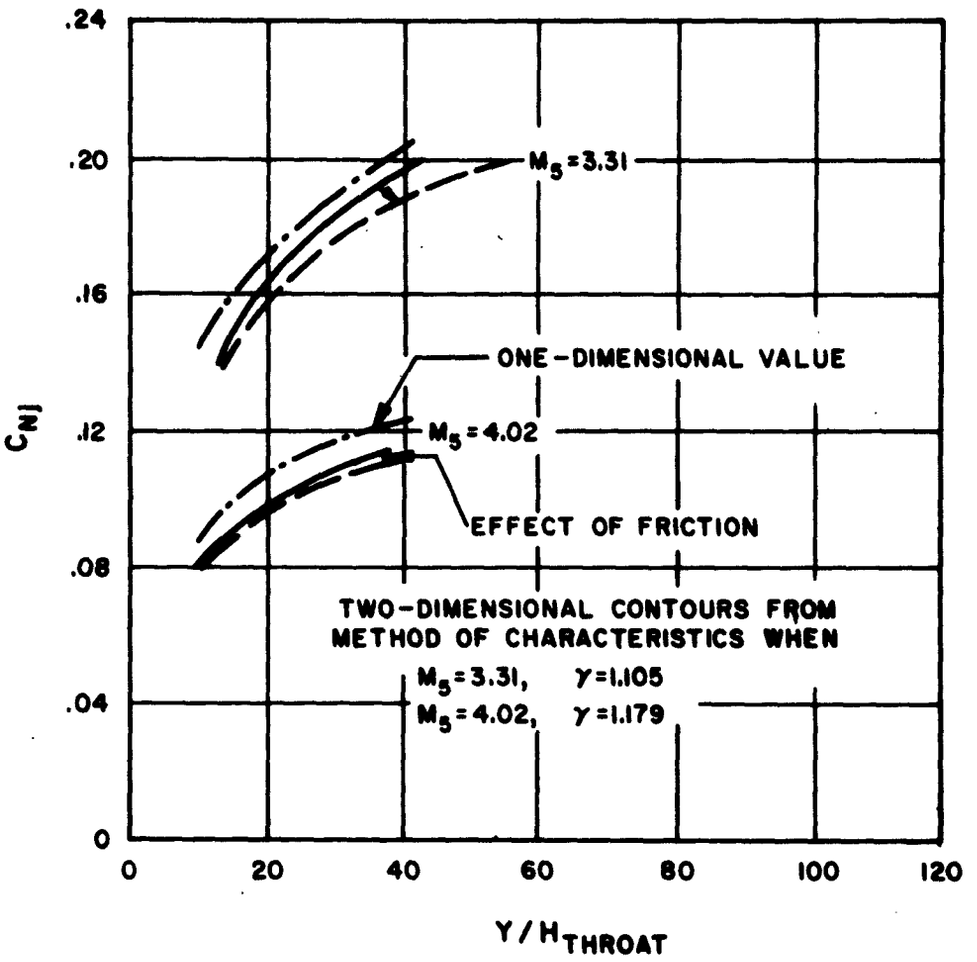

FIGURE 5.7
NOZZLE IMPULSE COEFFICIENT VS EXPANSION RATIO

5.5 EFFECT OF NONUNIFORM CONDITIONS AT NOZZLE ENTRANCE

The impulse of the exhaust gases at the nozzle exit would depend upon the entrance flow conditions. Holding the value of j_5 the same, the nonuniform conditions at the nozzle entrance can be examined in terms of exit impulse. Thus, the effect of combustor exit conditions are accounted for in the nozzle performance instead of the combustor performance. Since the nonuniformities could result in nonisentropic and nonisenthalpic flows with a certain amount of mixing, any rigorous solution of the problem is not feasible. Also, it is not possible to consider parametric variation of nozzle configuration with parametric variation of entrance conditions. However, examination of nozzle flows, with a few suitably prescribed entrance conditions, can yield an indication of the influence of nozzle entrance nonuniformities.

For the purpose of studies reported here a nozzle configuration of $(L/Y_5) = 100$ and $(Y_6/Y_5) = 25$ is chosen. This is one of the family of nozzle contours designed for uniform entrance conditions with $M_5 = 4.02$ and $\gamma = 1.179$ and is shown in Figure 5.8. From the flow analysis by the method of characteristics, the entire flow field in the nozzle is known. In order to apply the "stream-tube" method for the study of nonuniformity effects, the nozzle entrance section is divided into three equal stream tubes, each passing equal amounts of mass flow. Utilizing the flow field computed for $\gamma = 1.179$, stream lines are drawn, as shown in Figure 5.8, separating the nozzle flow into three stream tubes, referred to as a, b, and c, in the following discussions. The exit flow of the nozzle configuration is nonuniform. For example, the static pressures P_6 across

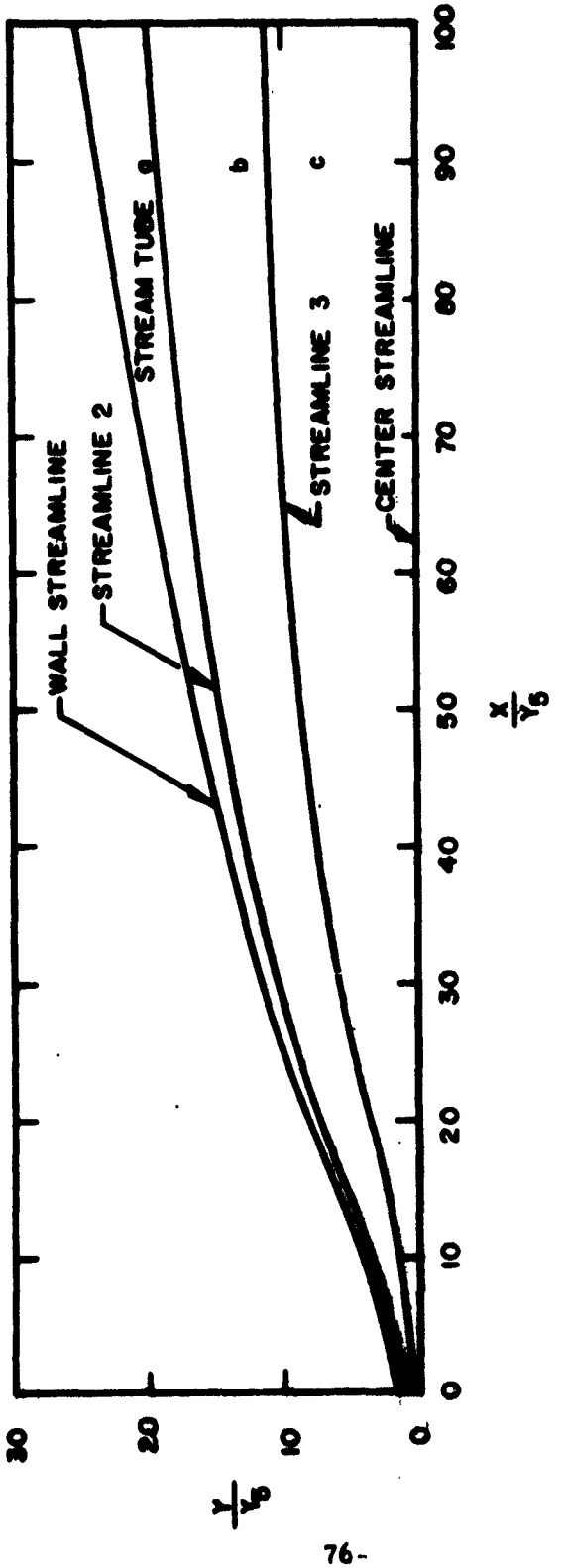

FIGURE 5.8
STREAM LINE LOCATIONS IN THE OPTIMUM THRUST NOZZLE ($(M_5 = 4.02, \quad = 1.179, \frac{L}{Y_5} = 100$
$\frac{Y_6}{Y_5} = 25$)

the nozzle exit are nondimensionalized to entrance station pressure P_5 and exhibit a distribution as shown in Figure 5.9. The exit flow of the nozzle is not axial and the flow directions measured from the axial direction are shown in Fig. 5.10. It should be remembered that the information presented in Figures 5.8 to 5.10 is obtained from field computed for $\gamma = 1.179$ and uniform nozzle entrance Mach number $M_5 = 4.02$.

In evaluating nozzle exit flow condition for nonuniform entrance conditions the "stream-tube" method of analysis is employed. Two typical cases of nonuniform conditions are assumed at the nozzle entrance and the resulting exit flow impulses are compared with the case of uniform entrance flow. The pressure and gas velocity at the nozzle entrance for all three cases are held the same and considered uniform. Fuel mass fraction is varied between the stream tubes, keeping the total fuel mass fraction the same. The various flow parameters assumed in the three stream tubes at the nozzle entrance are described in Table 5.1.

In evaluating the flow conditions at the nozzle exit the following assumptions are made:

1. One-dimensional flow in each stream tube without any mixing between adjacent stream tubes.
2. The expanding gases are in chemical and thermodynamic equilibrium in each stream tube.
3. The cross-sectional areas of the stream tubes at the nozzle exit projected on the exit plane normal to the axis, as shown in Figure 5.11, sum up to the nozzle exit area.
4. The variation of static pressure across the nozzle exit as obtained from stream tube analysis is similar to that obtained in the case of

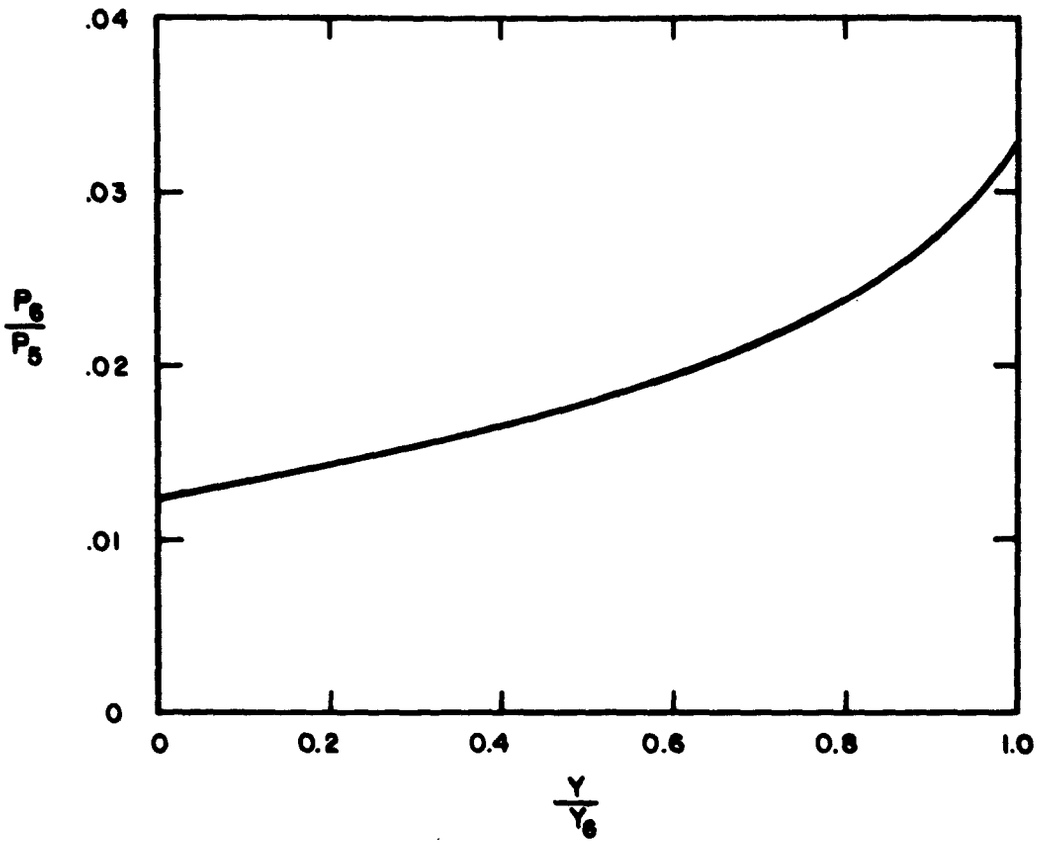

FIGURE 5.9
STATIC PRESSURE VARIATION AT THE NOZZLE SHOWN IN FIGURE 5.8

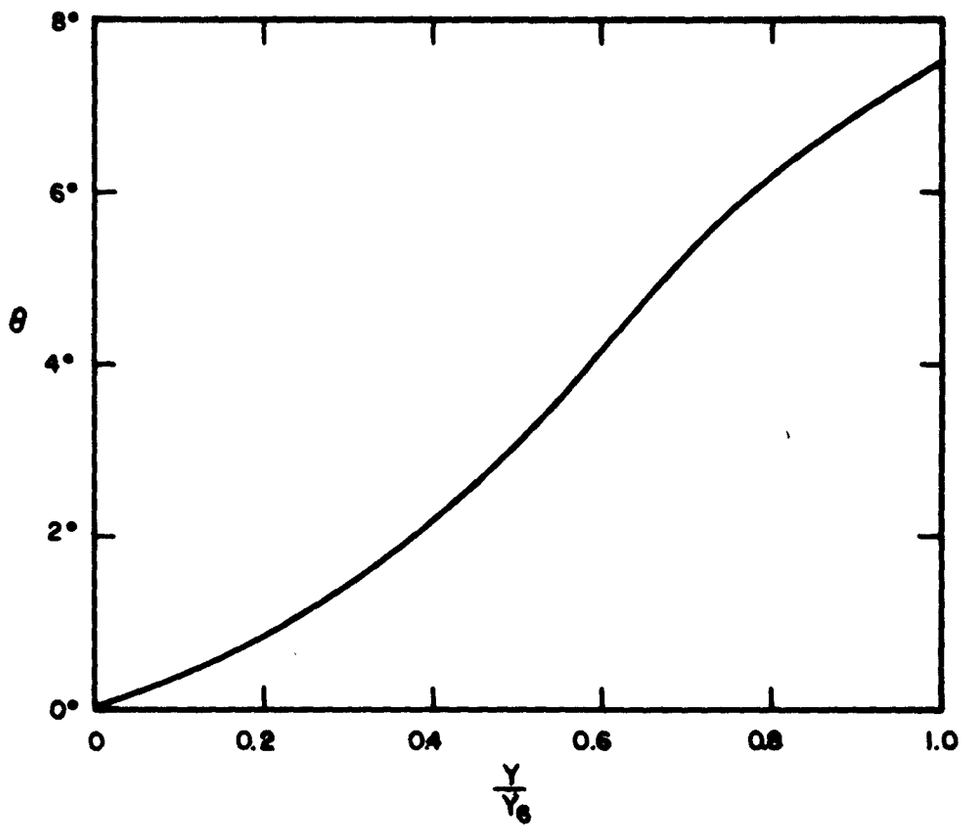

FIGURE 5.10
VELOCITY DIRECTIONS AT THE EXIT OF THE NOZZLE SHOWN IN FIGURE 5.8

TABLE 5.1

FLOW CONDITIONS ASSUMED AT THE NOZZLE ENTRANCE

	Stream-Tube a	Stream-Tube b	Stream-Tube c
cross-section	$\frac{Y}{Y_5}$ = 0.6667 to 1.0	$\frac{Y}{Y_5}$ = 0.3333 to .6667	$\frac{Y}{Y_5}$ = 0 to 0.3333
pressure	0.444_6 atm	0.444_6 atm	0.444_6 atm
velocity	0.7117×10^6 cm/sec	0.7117×10^6 cm/sec.	0.7117×10^6 cm/sec.
Case 1			
temperature	3148°K	3148°K	3148°K
fuel mass fraction	0.02833	0.02833	0.02833
Case 2			
temperature	3061°K	3148°K	3237°K
fuel mass fraction	0.042495	0.02833	0.014165
Case 3			
temperature	3237°K	3148°K	3061°K
fuel mass fraction	0.014165	0.02833	0.042495

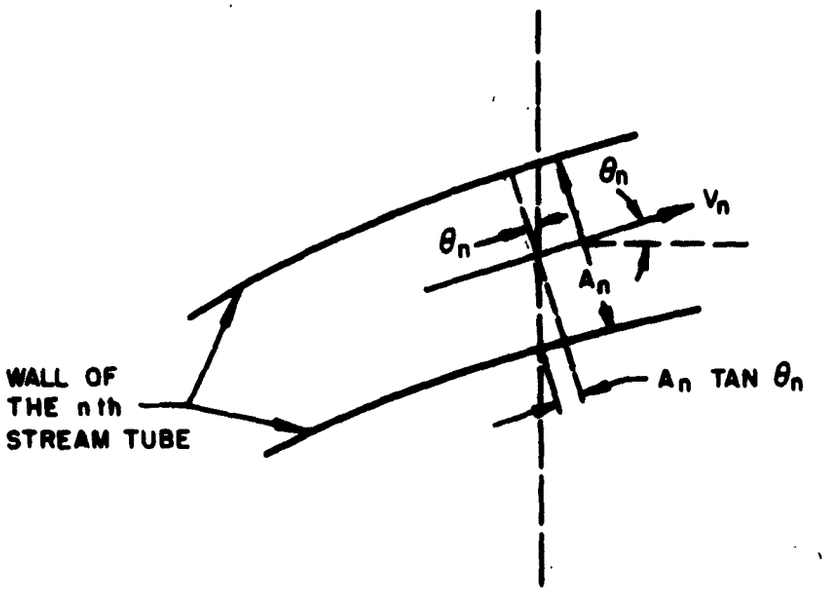

$$\dot{m}_{n\,in} = P_n A_n \left(1 + \frac{\rho_n V_n^2}{P_n}\right) \cos\theta_n + P_n A_n \tan\theta_n \sin\theta_n$$

LATERAL FORCE FROM nth STREAM TUBE =

$$-P_n A_n \left(1 + \frac{\rho_n V_n^2}{P_n}\right) \sin\theta_n + P_n A_n \tan\theta_n \cos\theta_n$$

FIGURE 5.11
SKETCH OF FLOW CONDITIONS IN THE N-TH STREAM TUBE AT NOZZLE EXIT

γ = 1.179 and shown in Figure 5.9, i.e., even though (P_6/P_5) values are not the same as shown in Figure 5.9, the variation of P_6, as denoted by (P_6/P_{6w}) is the same. The subscript w indicates the value of P_6 at the nozzle wall.

5. The flow directions of the stream tubes at the nozzle exit are the same as those obtained in the flow field computed for γ = 1.179 and shown in Figure 5.10.

The evaluation of flow conditions in the stream tubes at the nozzle exit is carried out by an iterative process because of the stipulation that the total cross-sectional area at exit is equal to Y_6. After determining the pressures, densities, and gas velocities in the respective stream tubes one can evaluate the exit impulse function as

$$j_6 = \frac{1}{\dot{m}} \left[\sum_{n=a,b,c} \left\{ \left(\dot{m}_n V_{6n} + P_{6n} A_{6n} \right) \cos\theta_{6n} + P_{6n} A_{6n} \tan\theta_{6n} \sin\theta_{6n} \right\} - \text{wall friction drag} \right] \tag{5.9}$$

The subscript n refers to the n^{th} stream tube, subscript 6 refers to the nozzle exit location, and θ denotes the direction of stream tube measured from the nozzle axis. $\dot{m}$ is the total mass flow through the nozzle. A_n is the cross-sectional area of the n^{th} stream tube, which in the two-dimensional case can be replaced by Y_n. The condition of prescribed value of exit area is satisfied by requiring

$$\sum_{n=a,b,c} \frac{A_{6n}}{\cos\theta_{6n}} = A_6 \tag{5.10}$$

The wall friction drag in the above Eq. (5.9) is assumed to be at the same value as computed for nozzle flow field obtained for γ = 1.179.

In a similar manner one can determine the value of j_5 which is simpler because the flow is axial and the nonuniformities are only in gas density. The nozzle impulse coefficient C_{Nj} computed for the three cases under consideration are given in Table 5.2. It should be noted that the C_{Nj} values shown parametrically in Figure 5.6 are the results of computations for constant $\gamma = 1.179$, whereas the value shown for Case 1 in the Table 5.2 is for equilibrium flow. For the sake of comparison the value of C_{Nj} obtained for this nozzle from constant γ computations is also shown in the Table. The influence of nonuniformity at nozzle entrance on C_{Nj} is indicated in Table 5.2. To eliminate the direct influence of nozzle area expansion ratio, the values of j_6 are nondimensionalized to j_{6i}, the one-dimensional value for the area ratio 25. For the cases 1, 2, and 3 the value of j_{6i} is taken from one-dimensional equilibrium flow computation corresponding to uniform entrance conditions as in Case 1, and the ratios (j_6/j_{6i}) obtained are shown in Table 5.2. In comparing the results from constant γ calculation the value used for j_{6i} was taken from one-dimensional flow at $\gamma = 1.179$. The corresponding values of (C_{Nj}/C_{Nji}) are also shown in the table.

The results presented in Table 5.2 indicate that the loss in thrust due to the nonuniform entrance conditions of the Case 2 or Case 3 is the same. When we consider uniform entrance flow with equilibrium expansion, the influence of the particular nozzle contour and friction drag on the wall together amounted to a loss of 0.47 percent of one-dimensional exit impulse. On the other hand, similar evaluation based on $\gamma = 1.179$

TABLE 5.2

EFFECT OF NONUNIFORM CONDITIONS AT ENTRANCE OF NOZZLE CONFIGURATION OF FIGURE 5.8

	C_{Nj}	C_{Nj}/C_{Nji}	C_{Ej}
Uniform entrance conditions - Case 1	0.05752	0.92017	0.99530
Nonuniform entrance conditions - Case 2	0.05697	0.91137	0.99479
Nonuniform entrance conditions - Case 3	0.05697	0.91137	0.99479
Uniform entrance condition --one-dimensional nozzle	0.06251	1.0	1.0
Uniform entrance conditions--γ= 1.179 (from Figure 5.6)	0.1033	0.91424	0.99129
Uniform entrance conditions--one-dimensional nozzle, γ= 1.179 (from Figure 5.7)	0.11299	1.0	1.0

computations indicate a loss of 0.871 percent of one-dimensional exit impulse for $\gamma = 1.179$. The influence of the gas properties show up more pronounced on the net nozzle thrust as indicated by C_{Nj} values. For constant $\gamma = 1.179$ computations a value of 0.1033 is obtained of C_{Nj}, compared with only 0.05752 when we consider equilibrium flow.

5.6 LATERAL FORCES DUE TO NONUNIFORM ENTRANCE CONDITIONS

Depending upon the configuration of the combustion chamber and fuel injector the flow conditions at nozzle entrance could be nonuniform. These nonuniformities at nozzle entrance would affect the downstream flow field in the nozzle, giving us differences in stream thrust at the nozzle exit and consequently, different values of lateral loads. Variations in this lateral load will reflect as changes in vehicle total lift. For the purpose of this investigation the nozzle configuration and entrance conditions used in Section 5.5 are considered. Using the "stream tube" method of analysis and the assumptions listed in Section 5.5 the flow conditions at the nozzle exit section are determined. Even though the flow directions of the individual stream tubes at the nozzle exit are considered unaffected by the nozzle entrance nonuniformities, the changes in exit stream thrust of individual stream tubes yield changes in the lateral force on the nozzle. After evaluating the appropriate exit flow conditions the lateral force can be computed as

$$\frac{1}{\dot{m}} \sum_{n=a,b,c} \left\{ \left(\dot{m}_n V_{6n} + P_{6n} A_{6n} \right) \sin \theta_{6n} + P_{6n} A_{6n} \tan \theta_{6n} \cos \theta_{6n} \right\} \tag{5.11}$$

where the notation used is the same as that in Eq. (5.9). The lateral forces computed for nozzle entrance conditions, defined as Cases 1, 2, and 3 in Table 5.1 are shown in Table 5.3 after normalizing to j_{6i}. Although the lateral force is only a small fraction of exit stream thrust it is of the same order of magnitude as the nozzle net thrust, i.e., by comparing to C_{Nj} values. Hence, the changes in the lateral loads in Cases 2 and 3 from that in Case 1 are of significant value. If the nozzle entrance conditions are unsteady in nature, one can expect the lateral force on the nozzle also to be unsteady. Even though periodic variations in the net thrust of an SCRJ engine can be tolerated to some extent, periodic changes in the lateral force can be dangerous, affecting the flight dynamics and structural integrity of the engine. Solution of unsteady flow field in a two-dimensional nozzle is not feasible. Examination of results presented in Table 5.3 indicates that if the nozzle entrance conditions change periodically from Case 2 to that of Case 3, there could be periodic variations in lateral force with an amplitude of .004 times j_{6i}. Comparing with values of C_{Nj}, we find that the amplitude of lateral force variation can be 5.1 percent of net nozzle thrust, whereas the amplitude of variation of net nozzle thrust is only 0.96 percent (from Cases 2 and 3 in Table 5.3).

TABLE 5.3

LATERAL FORCES DUE TO NONUNIFORM ENTRANCE CONDITION

	C_{Nj}	$\frac{\text{Lateral Force*}}{j_{6i}}$
Uniform entrance, equilibrium flow-- Case 1	0.05752	-0.0673
Nonuniform entrance, equilibrium flow-- Case 2	0.05697	-0.0654
Nonuniform entrance, equilibrium flow-- Case 3	0.05697	-0.0694

* The computed lateral force is in the negative Y direction.

5.7 EFFECT OF NONEQUILIBRIUM FLOW

As the exhaust gases in an SCRJ engine expand through the exit nozzle, a certain amount of chemical recombination occurs among the constituent species of the gases. The amount of recombination that occurs depends upon the time-rate of the expansion process and the chemical kinetic rates of the various reactions that can take place among the various species in the exhaust gases. Because of the energy released during the chemical recombination, the exit momentum of the exhaust gases increases as a function of the amount of recombination that can occur. On the other hand, for a given nozzle configuration of prescribed area ratio and prescribed inlet flow conditions, the amount of recombination increases with the nozzle size, i.e., a linear dimension of the nozzle. The "sudden-freezing" concept as proposed by Bray in Ref. 5 and extended to the hydrogen air case by Kushida (Ref. 6) can easily be applied to evaluate the expansion process in a nozzle, hence the exit impulse. The validity of the "sudden-freezing" point concept in the exhaust nozzle performance analyses has been demonstrated by Westenberg (Ref. 7).

With complex chemical systems in exhaust nozzle flow there are several, rather than one, possible freezing points. In the method of Ref. 6, the freezing of the concentrations of the hydrogen atom H, the oxygen atom O, and the hydroxyl radical OH is examined. The freezing point furthest downstream in the stream tube is chosen as the freezing point of reaction. The freezing point functions are expressed

in the form

$$\left(\frac{-d\ln P}{ds}\right)_H = \frac{n^2}{V}\left\{\frac{K_1(OH) + 2K_2(H) + K_4(O)}{d\ln(H)/\bar{m} \,/\, d\ln P}\right\}_{eq}$$

$$\left(\frac{-d\ln P}{ds}\right)_O = \frac{n^2}{V}\left\{\frac{2K_3(O) + K_4(H)}{d\ln(O)/\bar{m} \,/\, d\ln P}\right\}_{eq}$$

$$\left(\frac{-d\ln P}{ds}\right)_{OH} = \frac{n^2}{V}\left\{\frac{K_1(H) - K_4\frac{(O)(H)}{(OH)}}{d\ln(OH)/\bar{m} \,/\, d\ln P}\right\}_{eq}$$

where k_1, k_2, k_3, and k_4 are the reaction rate coefficients listed in Table 5.4 for the four important recombination reactions in hydrogen-oxygen combustion. These functions are evaluated as part of an equilibrium expansion program and are independent of the nozzle size. At a given pressure condition the freezing point function with the largest absolute value is chosen as the critical one. In the present problem, the OH radical proved to be the most important. The values of $(-d\ln P/ds)_{OH}$ are shown on a log-log plot as a function of pressure in Figure 5.12 for various values of fuel mass fractions. The fuel mass fractions are normalized to the stoichiometric fuel mass fraction and are shown as equivalence ratios in Figure 5.12.

TABLE 5.4

REACTION RATES USED IN FREEZING POINT COMPUTATION

Reaction	Rate Coefficient $(cm^3/mole)^2/sec$
$H + OH \xrightarrow{M} H_2O$	$k_1 = 5.4 \times 10^{17}/T$
$H + H \xrightarrow{M} H_2$	$k_2 = 7.5 \times 10^{18}/T$
$O + O \xrightarrow{M} O_2$	$k_3 = 0.67 \times 10^{14}(4500/T)^{1.5}$
$H + O \xrightarrow{M} OH$	$k_4 = 1.0 \times 10^{15}$

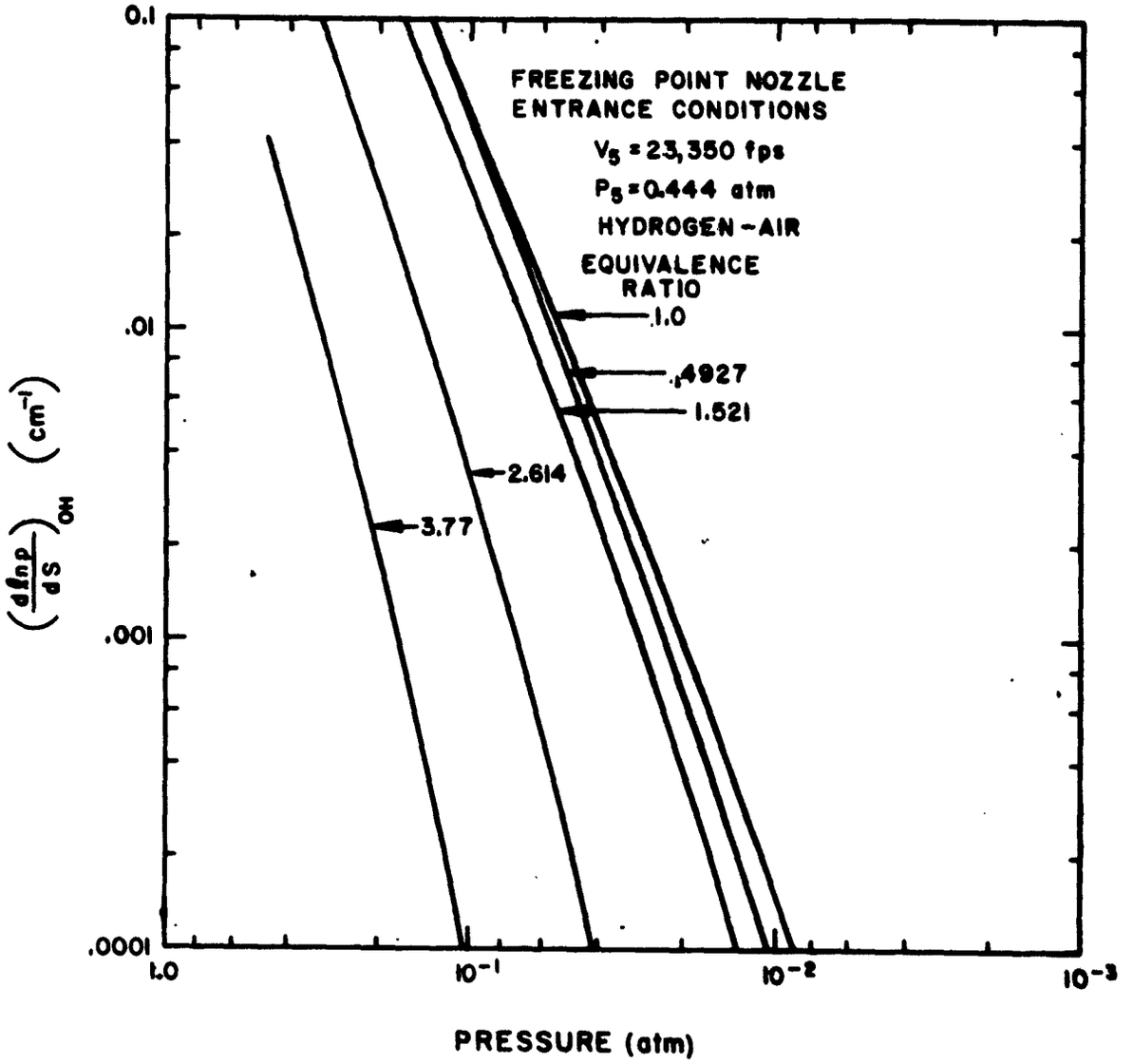

FIGURE 5: 12
CRITERION FOR EQUILIBRIUM IN THE NOZZLE FLOW

At any particular value of pressure P, if the expansion along a stream line in a nozzle produces a higher value of $-\frac{d \ln P}{ds}$ than indicated in Figure 5.12, the chemical reactions are considered frozen at that location. Subsequent expansion of the exhaust gases as they travel along the stream line can be computed with frozen chemical composition obtained at the "sudden-freezing" point.

For the investigations reported here, the nozzle configuration shown in Figure 5.8 is considered. From the known flow field previously computed for $M_5 = 4.02$ and $\gamma = 1.179$, two stream lines are shown in Figure 5.8. Including the nozzle wall and center line we have four stream lines along which the pressure variations are known from $\gamma = 1.179$ computation and are described in Figures 5.13a and 5.13b. For a particular size of the nozzle entrance, say $Y_5 = 1$ ft., the values of $-\frac{d \ln P}{ds}$ can be computed along these stream lines. These values for each stream line are shown in Figure 5.14, against pressure on a log-log plot. Comparing the conditions attained in the nozzle, as shown in Figure 5.14 with the "sudden-freezing" criterion, as shown in Figure 5.12, one can locate along each stream line the point downstream of which the expansion process can be assumed to occur with frozen composition, as shown in Figure 5.15. In evaluating the impulse at the nozzle exit the following assumptions are made:

1. The nozzle flow is divided into three stream tubes with no mixing occurring across the stream-tube walls.
2. One-dimensional flow is assumed in each stream tube, i.e., flow conditions are uniform across each stream tube even

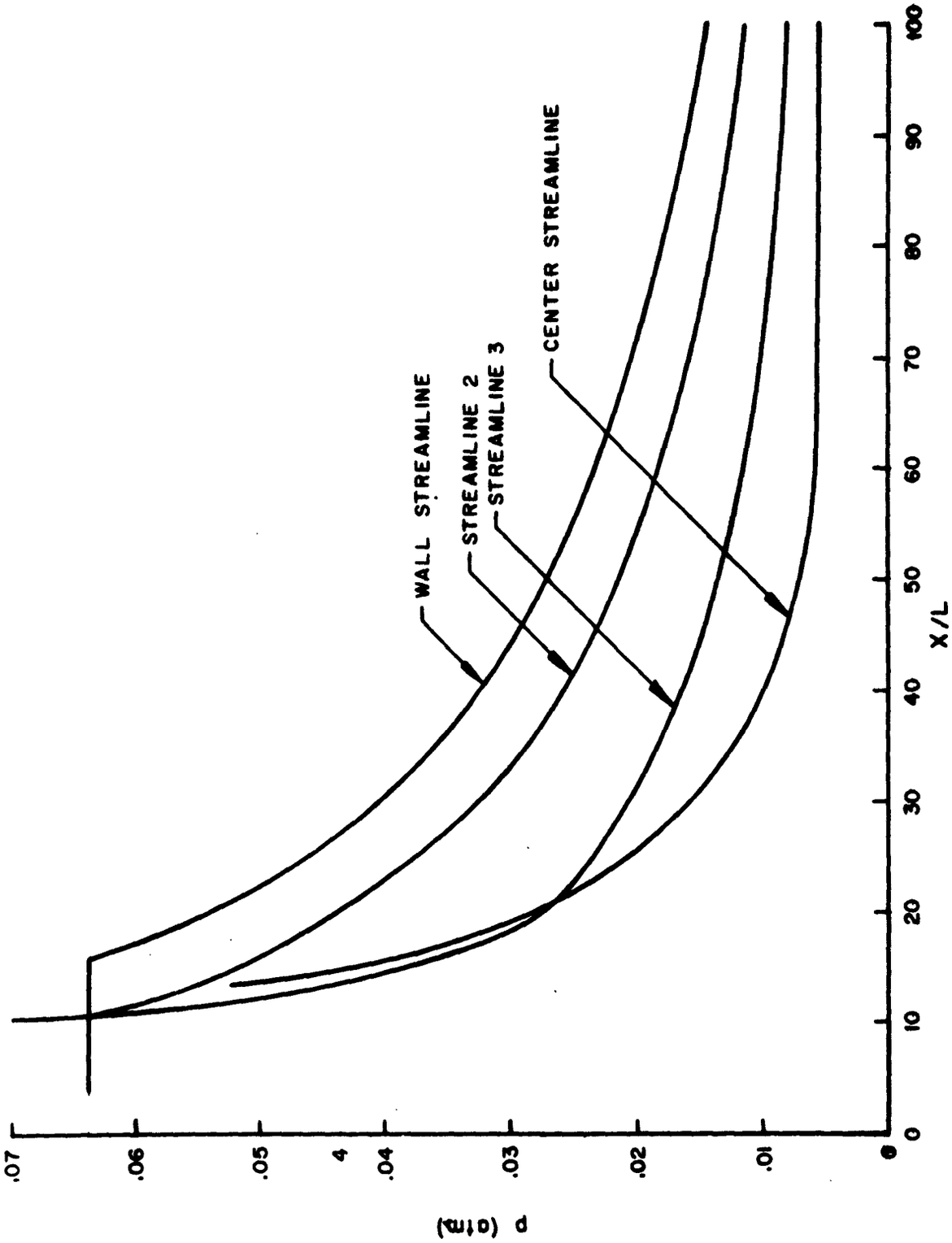

FIGURE 5.13a
PRESSURE VARIATIONS ALONG THE STREAM LINES IN THE FLOW FIELD ($\gamma = 1.179$) FOR NOZZLE SHOWN IN FIGURE 5.8

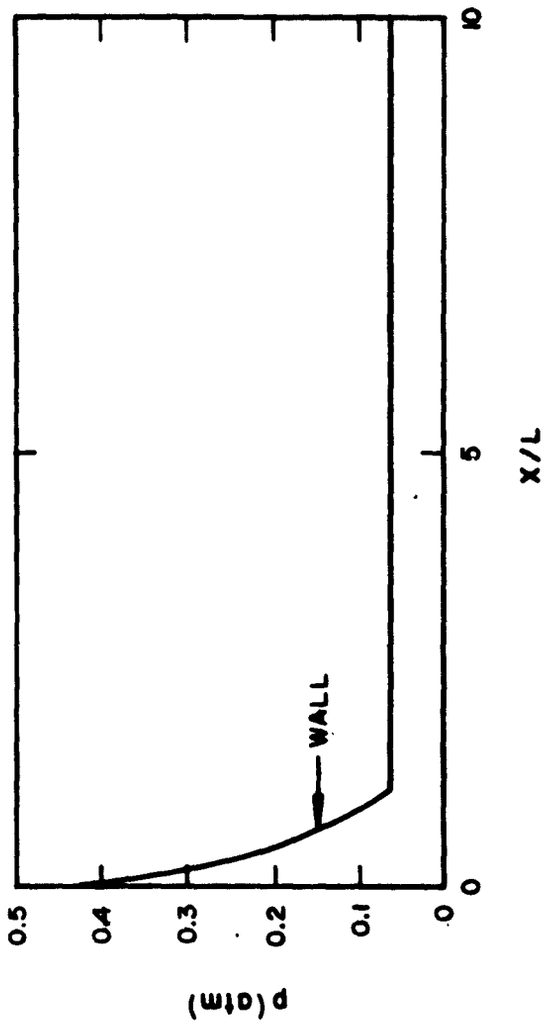

FIGURE 5.13b
PRESSURE VARIATIONS ALONG THE STREAM LINES IN THE FLOW FIELD ($\gamma = 1.179$) FOR NOZZLE SHOWN IN FIGURE 5.8

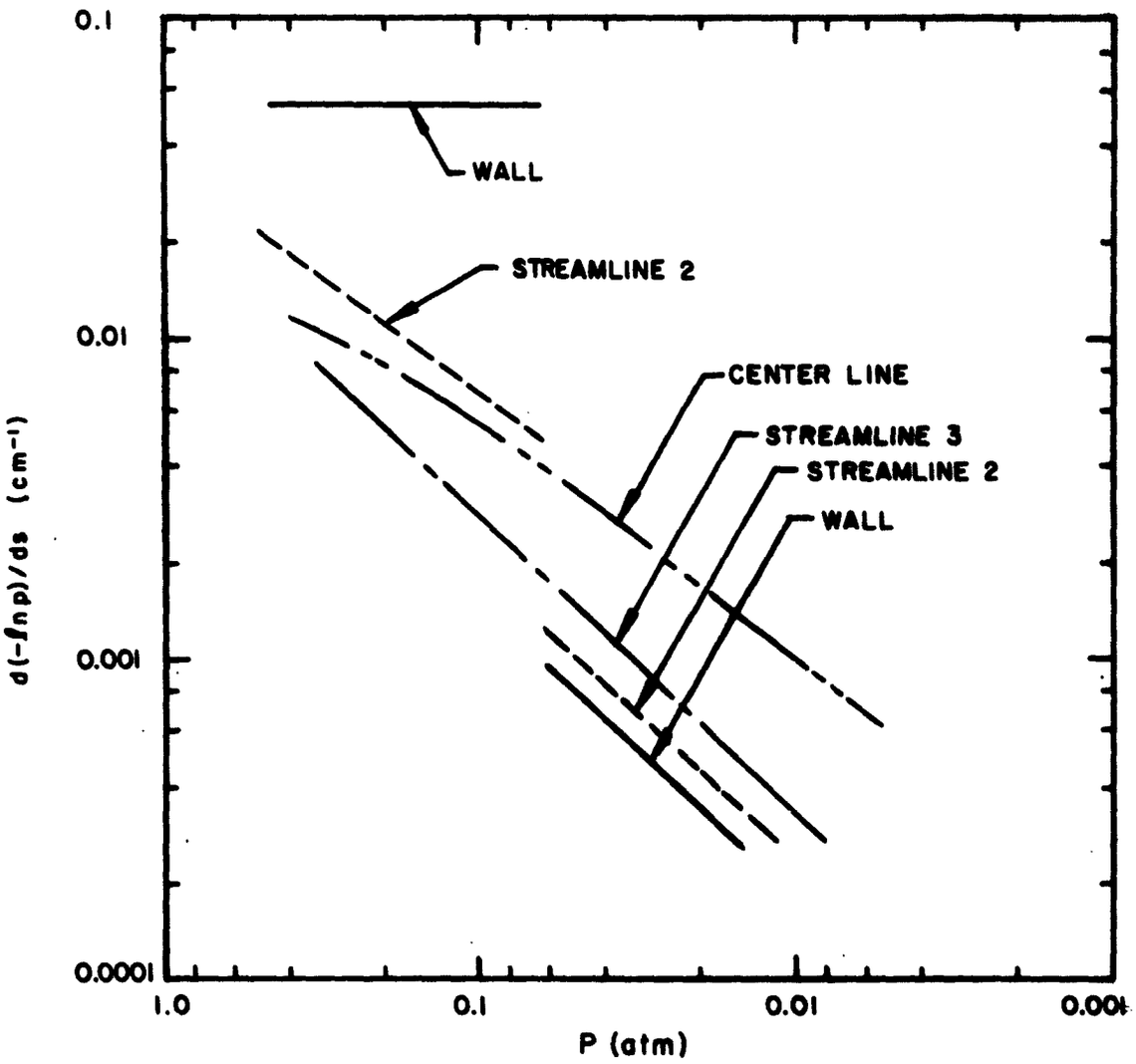

FIGURE 5.14
GRADIENT OF PRESSURE ALONG EACH STREAM LINE IN NOZZLE SHOWN IN FIGURE 5.8

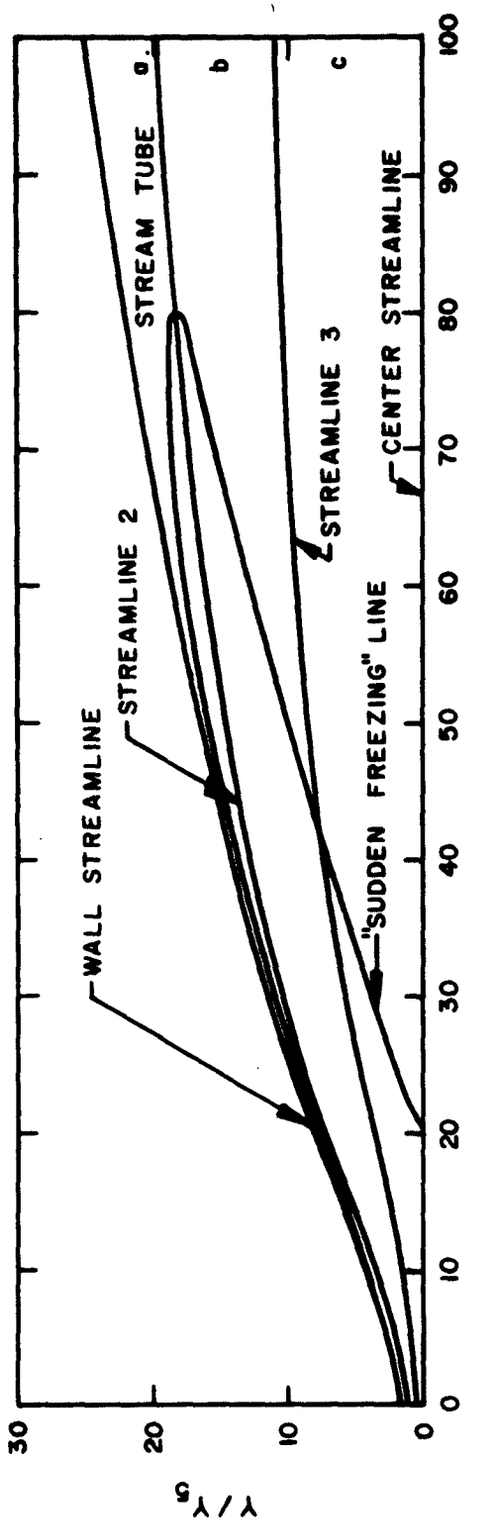

FIGURE 5.15
LOCATION OF 'SUDDEN FREEZING LINE" IN THE NOZZLE WITH Y_5 = 1 FOOT

though there could be variations between stream-tube to stream-tube.

3. Equilibrium expansion is assumed in each stream-tube up to the "sudden-freezing" line and subsequent expansion is considered to be with frozen composition. This location for "sudden-freezing" is described in terms of an average pressure across the stream-tube in our computations.

4. The pressures P_6 reached by the nozzle exit in each individual stream tube are such that the variation of the pressure P_6 across the exit section is similar to that obtained from the flow field computed for $\gamma = 1.179$ and shown in Figure 5.9.

5. The values of pressures in the stream-tubes are adjusted such that the sum total of the stream-tube cross-sections projected on the exit plane, as shown in Figure 5.11 are equal to the prescribed exit area A_6.

6. The velocity directions of the flow in the stream-tubes are assumed to be similar to the flow field computed for $\gamma = 1.179$ and shown in Figure 5.10.

As in the previous Section 5.5 the evaluation of flow conditions in the stream-tubes at the nozzle exit is carried out by an iterative process by satisfying Eq. (5.10) so that prescribed exit area A_6 is obtained. After determining the pressures, densities, and gas velocities in the respective stream-tube the exit impulse function j_6 is computed according to Eq. (5.9). Because the conditions at the nozzle entrance are assumed uniform the value of j_5 will be the same as that computed for Case 1 in Table 5.2. The nozzle impulse coefficient C_{Nj} and the exit impulse coefficient C_{Ej} computed for this

nozzle under the "sudden-freezing" assumption (referred to as Case 4 in following discussions) are shown in Table 5.5 and are compared with the values for equilirbium flow conditions.

TABLE 5.5

EFFECT OF INCOMPLETE RECOMBINATION IN NOZZLE CONFIGURATION OF FIGURE 5.8 - Y_5 = 1 ft.

	C_{Nj}	$\frac{C_{Nj}}{C_{Nji}}$	C_{Ej}
Equilibrium flow (Case 1)	0.05752	0.92017	0.99530
"Sudden-freezing" assumption (Case 4)	0.05648	0.90353	0.99432

The results reported here indicate that the losses due to incomplete recombination of exhaust gases in the nozzle configuration and size considered can be estimated to be 0.098 percent of j_{6i} by utilizing the "sudden-freezing" method. Even though this loss is small in terms of j_{6i} it can be a significant portion of net nozzle thrust, as can be observed from C_{Nj} values.

5.8 INTERACTION OF NOZZLE LOSSES

From the discussions presented in the previous subsections one can enumerate the various losses that can occur in a nozzle of prescribed area ratio and length.

1. Losses due to nonuniform exit flow (even in the case of optimum thrust contour the exit flow deviates considerably from one-dimensional value for the area ratio).
2. Losses due to wall friction on the nozzle wall and the heat transfer to nozzle wall.
3. Losses due to nonuniform conditions at the entrance to the nozzle.
4. Losses due to incomplete recombination of the exhaust gases.

The first item in the above is independent of nozzle size and to some extent depends upon the properties of the exhaust gases, such as an appropriate value of γ used for the expansion process. The latter three items can be evaluated only for a prescribed nozzle size and flow conditions in the nozzle.

The above itemized losses are influenced by each other and one can carry out the computations by suitable assumptions only for a given nozzle flow field, as described in detail in Sections 5.5 and 5.7. However, one can examine whether these losses can be computed individually so that tedious computations can be avoided. The following discussion pertains to checking the validity of adding up individual losses computed from quasi one-dimensional flows to obtain the combined loss in a given nozzle configuration.

The first of the various losses itemized above can be computed for a given nozzle configuration (area ratio and length) based on optimum thrust contour and an appropriate value of constant γ. For the nozzle

configuration described in Figure 5.8 this flow divergence loss is 8.58 percent of C_{Nji}, with C_{Nji} computed for $\gamma = 1.179$ and $(A_6/A_5) = 25$.

The second item, i.e., loss due to frictional drag on the nozzle wall was computed as 1.51 percent of C_{Nji}, based on wall conditions obtained from constant $\gamma = 1.179$ computations. One may say that minor variations of nozzle contour and equilibration of exhaust products would not alter the frictional drag loss appreciably, provided the linear dimensions are kept the same. The influence of heat transfer to nozzle wall is not considered in the present evaluation.

The last item, i.e., loss due to incomplete recombi nation can be easily evaluated for quasi one-dimensional flow at the nozzle exit. The exit flow of the nozzle can be assumed at uniform pressure and axial direction in place of preassigned distributions as in Figures 5.9 and 5.10. The flow through the nozzle is divided into three stream tubes as in Section 5.7 to obtain "sudden-freezing" locations in the individual stream tubes. However, uniform pressure is assumed at the nozzle exit and the condition of assigned value of A_6 is imposed. Because the amount of recombination occurring in each stream tube is different, the exit specific impulse is not uniform across the nozzle exit. The result of such computations shows that for the assumption of uniform pressure at the exit plane, the loss indicated for incomplete recombination is 1.55 percent of C_{Nji}.

TABLE 5.6

COMPARISON OF LOSSES ESTIMATED BY QUASI ONE-DIMENSIONAL ANALYSIS AND MORE EXACT ANALYSIS

(The losses denoted as percent of C_{Nji})

	Case 2	Case 4
Contour loss	8.58	8.58
Friction loss	1.51	1.51
Nonuniform entrance loss	0.66	0
Incomplete recombination loss	0	1.55
Estimated loss (Quasi one-dimensional)	10.75	11.64
Exact analysis (from Tables 5.2 & 5.5)	8.86	9.65

The third item, i.e., losses due to nonuniformities at nozzle entrance can also be evaluated in terms of one-dimensional exit flow. The approach taken is similar to the one described above except that equilibrium flow is assumed in each stream tube. The results of such computations, for the two types of nonuniform entrance conditions described as Cases 2 and 3 of Table 5.1 show that for the assumption of uniform exit pressure the loss due to nonuniform entrance conditions is 0.66 percent of C_{Nji}.

The various losses computed from quasi one-dimensional analysis are shown in Table 5.6. Let us consider the summation of the losses. For the nozzle flow conditions described as Case 2, the quasi one-dimensional estimates indicate a loss of 10.75 percent of C_{Nji} compared with a slightly lower value of 8.86 percent obtained from the more exact analysis. For the nozzle flow conditions described as Case 4 the quasi one-dimensional estimates indicate a loss of 11.64 percent of C_{Nji} compared with 9.65 percent obtained from the more exact analysis.

From the numerical computational results and discussion presented in this subsection, one can conclude that even though the losses in a nozzle depend upon the particular flow field, one can make conservative estimates from quasi one-dimensional computations.

5.9 LIFT FORCE DUE TO ASYMMETRIC CONFIGURATION

Asymmetric nozzle configurations have appeared with considerable frequency in supersonic combustion ramjet conceptual studies.

This is due partly to the problems involved with integrating the engine with an airframe and partly to the asymmetry of low loss inlets. A lateral force is generated by an asymmetric nozzle which, if the nozzle is properly oriented, will contribute to the vehicle lift.

One particular type of asymmetric nozzle was studied in Ref. 8. This was the one wherein the lower wall of a symmetric nozzle is cut back shorter than the upper. For this type asymmetry, the thrust and lift forces may be treated independently as long as the last left-running characteristic from the lower wall does not intersect the upper wall, as shown in Figure 5.16.

From the flow fields computed for constant γ in several uniform exit flow nozzles, the ratios of lift force to axial component of exit stream thrust, obtained for various amounts of lower wall truncation, are shown in Figure 5.17. The ambient pressure is assumed zero, giving us the lift force directly from the differential of pressure forces acting on the upper and lower walls.

To indicate the loss in thrust due to lower wall truncation, the changes in the exit stream thrust are shown in Figure 5.18. The specific curves (previously described in Ref. 8) obtained for each area ratio nozzle crossed one another, hence have been shown as a band for simplicity in both Figures 5.17 and 5.18. It should be remembered that the normalizing factor used in these figures is the exit stream thrust, whereas the net engine thrust will be only a fraction of this due to the inlet momentum drag. An examination of Figures 5.17 and 5.18 indicates that considerable amounts of lift

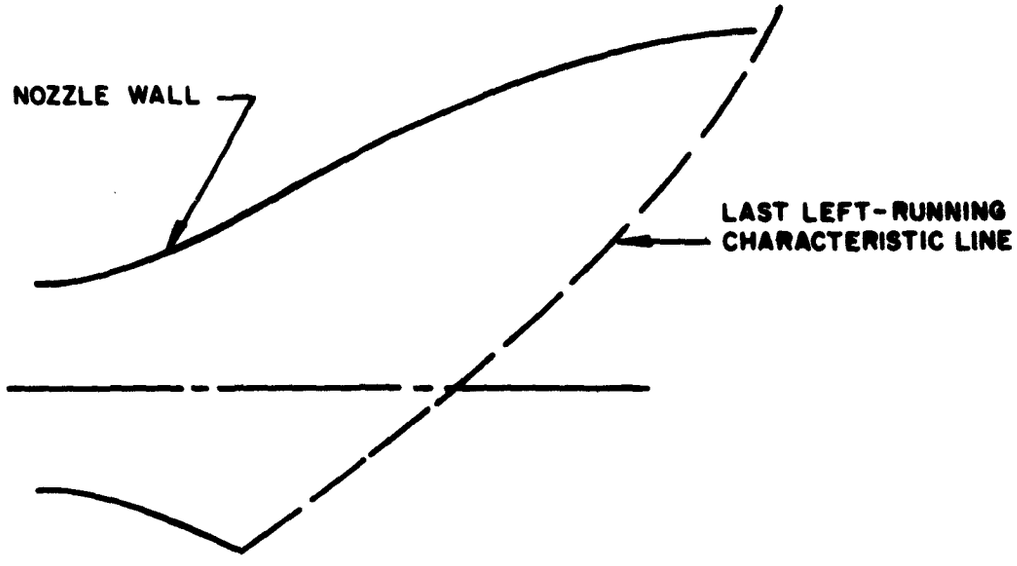

FIGURE 5.16
TRUNCATION OF LOWER WALL IN A TWO-DIMENSIONAL SYMMETRIC EXIT NOZZLE

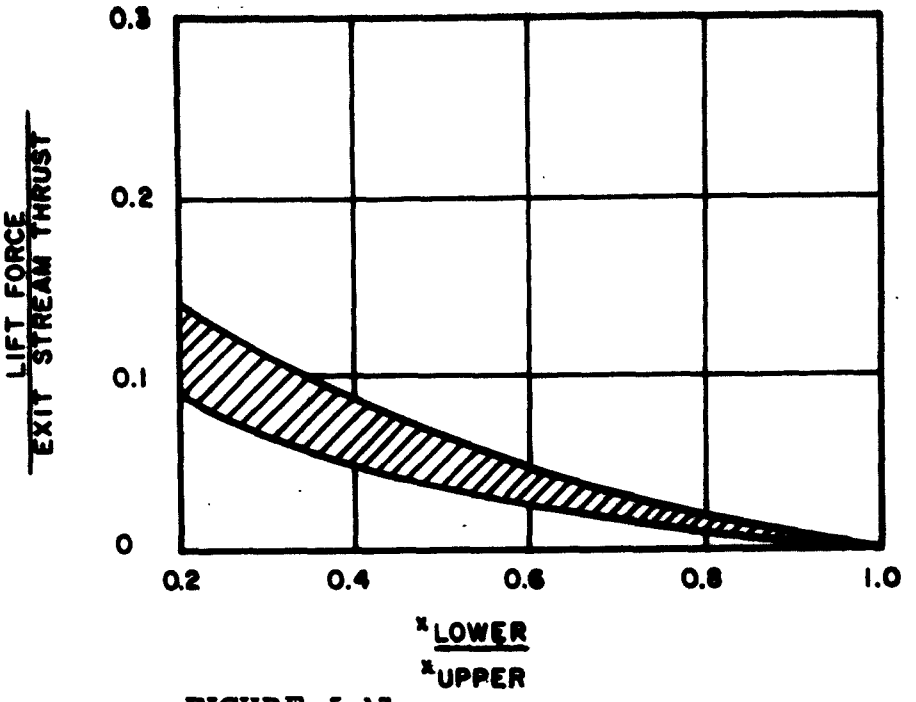

FIGURE 5.17
LATERAL FORCE DEVELOPED BY LOWER WALL TRUNCATION

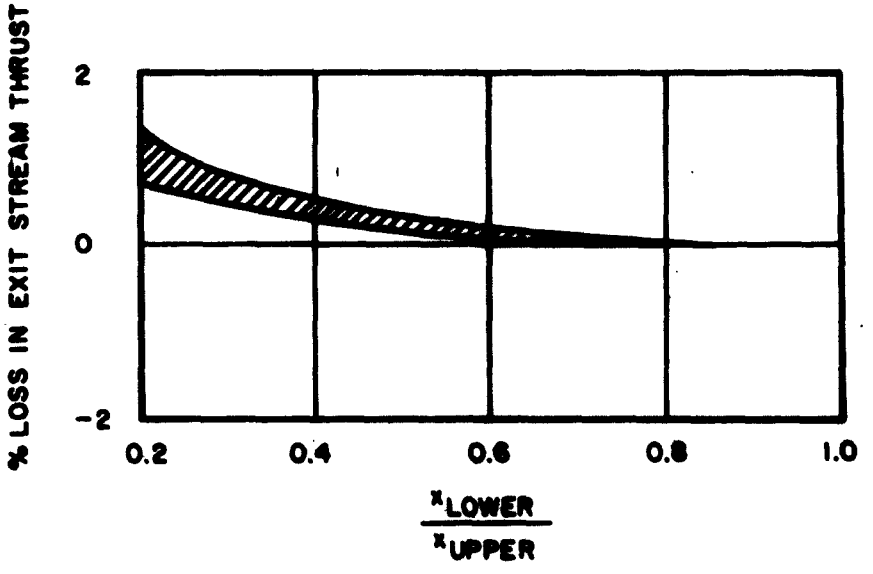

FIGURE 5.18
LOSS IN EXIT STREAM THRUST DUE TO LOWER WALL TRUNCATION

force can be obtained with negligible loss in thrust performance. Consideration of nozzle weight and envelope restrictions also would favor the use of lower wall truncation.

5.10 CONCLUSIONS

Based on the nozzle flow studies and the results presented here the following conclusions can be made.

1. Even minor gains in exit stream thrust are of significant importance in the case of an SCRJ engine exit nozzle, hence it is profitable to use nozzle configurations optimized for thrust.

2. The properties of exhaust gases employed in the analysis of nozzle flow (i.e., constant γ, or equilibrium flow assumptions) affects the nozzle impulse coefficient considerably.

3. Frictional drag on the nozzle wall is of significant value such that one finds an optimum length of a given nozzle area expansion ratio.

4. In evaluating the losses due to nonuniform entrance conditions or incomplete recombination within the nozzle, the assumptions made regarding the exit flow conditions play an important role.

5. The various losses in a nozzle attributable to different sources are interdependent and cannot be summed up from separate estimates. The sum total of the losses has to be evaluated

for the flow field occurring in the nozzle being examined.

6. Asymmetric nozzle configurations can profitably be employed to yield large amounts of lift force with negligible loss in nozzle thrust.

7. Nonuniform conditions at nozzle entrance yield lateral forces on the nozzle, which vary with the nature of the nonuniformity. For the particular types of nonuniformities studied, changes in the lateral force can be five times the changes in the net nozzle thrust.

5.11 RECOMMENDATIONS

The exit nozzle studies presented in this section and the limited number of computations carried out showed the need for further investigations in certain areas. Based on our studies the following items can be recommended for further examination to provide a sound basis for nozzle performance estimates.

1. When we consider nozzles of limited length, the exit flow is necessarily nonuniform and the consequent loss in thrust is a strong function of the exhaust gas properties used in the flow field analysis. One is tempted to use an appropriate constant value of γ. However, the particular choice of γ needs caution. For example, the flow divergence loss obtained for equilibrium flow does not apply for the case of flow with incomplete recombination. Further studies on the appropriate

choice of γ for evaluation of flow field is recommended.

2. In utilizing "stream-tube" method for evaluating the exit stream thrust of a nozzle of limited length, an assumption regarding the nature of the exit flow conditions is necessary. However, the results appear to depend upon the assumptions made. Further analytical and experimental effort is recommended to guide the investigator in the choice of the assumptions.

3. Periodic nature of lateral forces caused by periodic non-uniformities at nozzle entrance, require further study.

4. The use of "sudden-freezing" concept coupled with "stream-tube" method appears attractive for nozzle flow analysis in the case of incomplete recombination of exhaust gases. However, the validity of such an approach remains to be checked against detailed flow field computations utilizing the method of characteristics, incorporating finite rates of reactions among the species of the exhaust gases.

5. In the parametric study of optimum thrust nozzle configurations, it is not necessary to confine oneself to the use of constant γ. Provided the "sudden-freezing" concept is valid, the last characteristic line (in most cases) would lie in the region of flow with frozen gas composition. Rao's method can then be applied and the contour optimization can be extended to cover nozzles where recombination is incomplete. Further investigation of this approach is recommended.

5.12 REFERENCES

1. Rao, G. V. R., "Exhaust Nozzle Contour for Optimum Thrust," Jet Propulsion, Vol. 28, No. 6, June 1958.

2. Moore, M., Seiveno, D. H., "Description of a Program for the Design and Analysis of Supersonic Nozzles," Technical Report No. 129-3, National Engineering Science Co., Pasadena, California, August 1964.

3. Kushida, R., Seiveno, D. H., and Tromblay, J., "Advanced Air-Breathing Engine Study (U)", Technical Doc. Rept. No. APL-TDR-64-16, Second Qtrly. Rept. on Contract No. AF 33(657)-10794, National Engineering Science Co., Pasadena, Calif., April 15, 1964. CONFIDENTIAL REPORT

4. Kushida, R., et al, "Analytic Investigation of Advanced Air-Breathing Engines (U)", Technical Doc. Rept. No. ASD-TDR-62-856, Mid Term Report on Contract No. AF 33(657)-9244, National Engineering Science Co., Pasadena, Calif., December 21, 1962. CONFIDENTIAL REPORT

5. Bray, K. N. C., "Atomic Recombination in a Hypersonic Wind Tunnel Nozzle," Journal Fluid Mechanics, 6, 1959, pg. 1.

6. Kushida, R., "Nonequilibrium Recombination Effects in Exhaust Nozzle Flow," Progress in Astronautics and Rocketry, Vol. 2, 1960.

7. Westenberg, A. A., & Favin, S., "Nozzle Flow with Complex Chemical Reaction," CM-1013, Johns Hopkins Univ., Applied Physics Lab, March 1962.

8. Kushida, R., et al, "Advanced Air-Breathing Engine Study (U)," Technical Doc. Rept. No. ASD-TDR-1093, Final Report on Contract AF 33(657)-9244, National Engineering Science Co., Pasadena, Calif., April 1963. CONFIDENTIAL REPORT